UNIVERSITY OF OKLAHOMA

GRADUATE COLLEGE

CATALYTIC UPGRADING OF SUGAR DERIVATIVES

A THESIS

SUBMITTED TO THE GRADUATE FACULTY

in partial fulfillment of the requirements for the

Degree of

MASTER OF SCIENCE

By

DIKEN HEMANT JAIN
Norman, Oklahoma
2016

CATALYTIC UPGRADING OF SUGAR DERIVATIVES

A THESIS APPROVED FOR THE
SCHOOL OF CHEMICAL, BIOLOGICAL AND MATERIALS ENGINEERING

BY

_____
Dr. Daniel Resasco, Chair

_____
Dr. Steven Crossley

_____
Dr. Lance Lobban

Dedication

To my parents and my sister.

Thank you for your love, support, encouragement and sacrifices

Acknowledgements

First and foremost, I would like to thank my parents and my sister for their support and constant encouragement. There have been difficult times during my research. I would lose confidence in myself and thought of giving up. But my family would help me in restoring my faith in hard work and persistence. With their help I would get back to doing research with same enthusiasm and vigor.

Secondly, I would like to thank my research advisor Dr. Daniel Resasco for his thoughtful comments for my research and motivating me during tough times. He always believed in my potential and never gave up on me. He would also ensure that my academic progress is satisfactory. I consider myself fortunate to be guided by one of the finest professor. There is always something new to learn from him.

I also want to acknowledge Dr. Steven Crossley and Dr. Lance Lobban for their advice for my research. A special mention goes to Dr. Tawan Sooknoi for helping me to overcome difficulties with my research.

Additionally, I would like to thank my colleagues Daniel Santhanaraj, Tuong Bui, Nhung Duong, Felipe Anaya, Zheng Zhao, Nick Briggs, Anvit Vartak, Rajiv Reddy Janupala and Talita Souza Castro for helping me clear my conceptual doubts and for their valuable insight.

I would like to thank all my friends Rishabh Jain, Maulin Gogri, Tarek Firoze Akhtar, Nauman Khan, Soham Pandya, Abhijeet Cholkar and Fatema Kheda, for bringing laughter and making the journey at OU a memorable one. A special mention goes to Anvit Dinkar Vartak, a good friend and officemate, for his humor, guidance, encouragement, and making my experience a cheerful one.

I would also like to extend my gratitude to Department of Energy for research funds and CBME department at OU for allowing me to purse my master's degree. A special thanks goes to CBME department staff for their assistance.

Table of Contents

List of Tables

List of Figures

Abstract

With industrial revolution there has been a huge increase in demand for petroleum-based fuel. Detrimental effects on environment due to unprecedented use of fossil fuels and shortage in its availability has spurred the search for renewable and low carbon emission fuels. Solution is provided in the form of lignocellulosic biomass. It has helped in reducing human dependence on fossil fuels, it is carbon neutral and it is a continuous source of energy. However, lignocellulosic biomass cannot be used in its present form. Need is to convert the biomass into fuel that is convenient to use, robust and efficient. Thermochemical conversion technology has shown promising results in conversion of lignocellulosic biomass to bio-oil. Multistage pyrolysis is one of the thermochemical processes giving high yield of bio-oil. Analyzing all the fractions of multistage pyrolysis process it is found that the yield of levoglucosan was highest as compared to all the other compounds. Hence, there is a need to convert levoglucosan to a valuable compound.

In this present contribution, upgrading strategy of levoglucosan is investigated. Shortcoming of upgrading a sugar derivative and measures taken to overcome them have been discussed. Efforts to find compounds which can either directly act as fuel or as intermediates in production of fuels, have been carried out. Various catalyst systems have been tested for this purpose. 5 wt.% Pd/MWCNT was able to convert glucose to cyclic ketones in a single pot reaction. Cyclic ketones can undergo aldol condensation to form diesel range products. An attempt has been made to optimize the reaction conditions to get highest yield of products.

We can also derive numerous chemical building blocks from biomass. These building blocks either supplement or replace current supply of petroleum-derived chemicals. In the later part, we discuss the upgrading strategy of furfural to 1,5-pentanediol, which finds application as polyester and plasticizer. Furfural is hydrogenated on bimetallic catalyst like Cu/Ni to tetrahydrofurfuryl alcohol (THFAL). THFAL is converted to 1,5-pentanediol by direct hydrogenolysis or by a multi-step process. We intend to develop a bifunctional catalyst which is able to carry out multi-step process in a single pot reaction. We investigate different catalyst systems and solvents, to get high yield of 1,5-pentanediol. Cu/SiO_2-Al_2O_3 was able to convert 3,4 dihydropyran to 1,5 pentanediol with a yield of 80% in 3 hrs. Using tetrahydrofurfuryl alcohol as feed and MCM-41-SO_3H-PTS as catalyst a combined product yield (3,4 dihydropyran and δ-hydroxyvaleraldehyde) of 21% is attained in 2 hrs.

Chapter 1: Literature Review

1.1. Introduction

Fossil fuel has transformed the way mankind carries out their day to day activities. A major transformation is seen in transportation, manufacturing industries, and power generation. A number of consumer products are obtained from fossil fuels. They have high energy density and low moisture content. All these factors have led to an unprecedented use of fossil fuels and hence, there has been a major concern about its availability. More than the availability, the major concern is the impact that fossil fuels have on the environment. Fossil fuel emits CO_2, a greenhouse gas, which is believed to be the root cause of global warming [1]. Also, these fuels are a non-renewable source of energy. A report by ExxonMobil has estimated that the energy demand will increase by 35% by 2040 [2]. All these factors have stimulated the search for cleaner fuels, which can complement present source of energy to meet energy demand. Biomass upgrading has offered a renewable and sustainable solution. Nature produces 200 billion metric tons of biomass with an energy content of 3×10^{18} KJ per year by photosynthesis, which is around 10 times the present and annual energy consumption of the world [3]. The net emission of CO_2 from biofuels is less as compared to fossil fuels. Life cycle analysis completed by the National Renewable Energy Laboratory, and later by Argonne National Laboratory, found that greenhouse gas emission from 100% biodiesel could be more than 52% lower than those from petroleum diesel [4].

There are various sources of biomass such as wood products, dried vegetation, crop residue to name a few. Biomass is made up of hemicellulose (17 to 35%), cellulose (28 to 55%) and lignin (17 to 35%) [5].

We cannot use biomass in its original form as it has high oxygen content, it is hydrophilic, has low calorific value, low energy density and has high moisture content [6]. Hence, an upgrading strategy is required for converting biomass into biofuel. The most common and inexpensive upgrading strategy employed is converting biomass to bio-oil by fast-pyrolysis and further catalytically upgrading bio-oil. Fast-pyrolysis is thermal decomposition process at high temperature in the absence of oxygen. It produces a complex mixture of over few hundred oxygenated compounds [5]. Bio-oil is a very complicated mixture with low heating value, highly unstable, selective towards polymerization and corrosive. Hence, bio-oil needs to be stabilized. Moreover, the typical vapor-phase upgrading used in conventional petrochemical processes is more difficult with carbohydrates due to their low vapor pressure and poor thermal stability [7]. Therefore, liquid phase upgrading appears as a necessary approach for these feedstocks [8]. Due to the complexity of bio-oil, we cannot apply a single catalytic upgrading process. Hence, it is very important to separate bio-oil in different fractions of the same class of compounds and apply a suitable upgrading strategy to each class. There are two approaches to producing bio-oil with different fractions: 1) pyrolyze biomass and condense vapors at different temperatures 2) pyrolyze biomass at different temperatures to get different fractions.

Oak tree wood has one of the most complex structure of biomass. It is subjected to multistage pyrolysis where thermal degradation of each constituent takes place at three different temperatures as shown in figure 1. Hemicellulose is the most reactive components and it decomposes at 225-325° C; cellulose is the most stable polymer with

the degradation range of 300-400° C. The rate of degradation of lignin is slower at low temperatures due to its low activation energy, generally increasing at temperature above 375° C. We get three fractions of bio-oil. The first fraction is made up of light oxygenates,

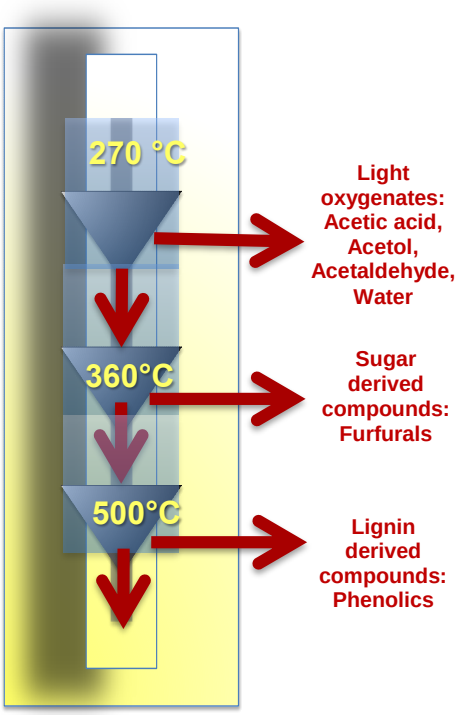

	Multistage pyrolysis of 10 kg oak tree				Single Stage Pyrolysis
Stage	1	2	3	Total	
H_2O	1.01	0.68	0.00	**1.69**	1.32
Acetic Acid	0.69	0.19	0.05	**0.93**	0.84
Acetol	0.31	0.19	0.18	**0.68**	0.91
Acetone	0.00	0.00	0.00	**0.00**	0.00
Furan	0.00	0.02	0.01	**0.03**	0.03
Furfural	0.14	0.41	0.07	**0.62**	0.50
Levoglucosan	0.02	0.76	0.48	**1.26**	1.84
Toluene	0.00	0.08	0.03	**0.11**	0.03
Guaiacol	0.18	0.21	0.15	**0.54**	0.58
Cresol	0.00	0.12	0.05	**0.17**	0.11
CO_2	0.72	0.85	1.15	**2.72**	2.43
Sum	3.07	3.50	2.17	8.75	8.58
			Char	1.25	1.42

Figure 1: Schematic representation of multistage pyrolysis process. Composition of all the three fraction are shown in the table on right hand side.
*Work done by Tyler Vann

the second fraction has sugar derived compounds and the third fraction is composed of lignin-derived compounds. The compositional analysis of each fraction of bio-oil for 10 kgs. of oak tree fed to multistage pyrolysis process is as shown in figure 1. We see that levoglucosan is in major proportion as compared to all other constituents. Hence, upgrading levoglucosan is imperative. Levoglucosan is formed by cleavage of glycosidic bond of cellulose.

Numerous chemical building blocks are derived from biomass which helps in supplementing or replacing petroleum-derived chemicals and fuels. For example,

levulinic acid can be employed in the production of chemicals such as diphenolic acid and δ-aminolevulinic acid as well as fuels such as meythyltetrahydrofuran, levulinate esters, and γ-valerolactone [9]. Furanic compounds are promising intermediates in the production of non-petroleum-derived chemicals because other biomass-related raw materials usually have a much higher oxygen content [10]. One of the basic non-petroleum chemicals accessible from biomass resource is furfural produced from acid catalyzed dehydration of pentoses [10]. In second part of thesis we discuss the upgrading strategy of furfural to 1,5-pentanediol, which acts as a precursor to δ-valerolactone. Furfural is starting material for manufacture of Tetrahydrofurfuryl alcohol (THFAL) by hydrogenation. THFAL can be converted to 1,5-pentanediol by two different methods. The first method is direct hydrogenolysis of THFAL over Rh-MoO/SiO_2, producing 1,5-pentanediol and 1,2-pentanediol as products. Second method is a multi-step process, with 3,4 dihydropyran and δ-hydroxyvaleraldehyde as intermediates. Work has been done to perform each step in a different reaction system. We plan to develop a bifunctional catalyst which can perform all the three steps in a single pot reaction. We test different catalyst system and solvents for this purpose. 1,5-pentanediol is valued at US$ 1000/ton and has applications as plasticizer, polyester, production of hydrogen and hydrogen peroxide and in pharmaceutical industry [10]. It also acts as an intermediate in production of δ-valerolactone. δ-valerolactone is priced at US$ 19,000/ton and is used as starting material for cyclic lactems, as an intermediate for polylactones, pharmaceutical industry, and as crop protection composition [11]. Looking at the high value of end products, its numerous applications and reduction in processing steps and cost achieved, developing a catalyst system for the same is a promising project.

1.2. Levoglucosan to glucose

Levoglucosan can successfully be converted to glucose by acid hydrolysis process. It follows first order reaction kinetics [12]. In the presence of 500 mM H_2SO_4 in water at 110° C we get 100% conversion of levoglucosan to glucose in 70 mins [12]. Increasing the temperature by 10° C resulted in a two-fold increase in concentration [12]. Doubling the amount of acid has the same effect as increasing the temperature by 10° C [12]. For levoglucosan hydrolysis in dilute sulfuric acid, the activation energy was 114 kJ mol^{-1} and Arrhenius constant was 1.0×10^{10} [12]

The major problem associated with sulfuric acid is the separation of acid which increases the acidity of reaction mixture [13]. Low pH enhances polymerization activity of sugars. Moreover, the highly acidic mixture would increase corrosion rate in industrial scale system. A solid acid catalyst is not limited by these problems. For example, Amberlyst-15 is a strong polymer-based acid with high SO_3H density and very high activity for a range of reactions [13]. As reported by Daniel Resasco et. al., Amberlyst-15 has similar activity to H_2SO_4 for levoglucosan hydrolysis to glucose [13].

1.3. Glucose to 5-(hydroxymethyl)furfural

Due to the low solubility of carbohydrates in organic media, polar solvents such as water are required [14]. Water is a desirable solvent due to its relatively reduced cost and reduced environmental impact [8]. As shown in figure 2, glucose is isomerized to fructose over lewis acid catalyst in the aqueous phase. Dehydration of fructose over bronsted acid catalyst gives 5-(hydroxymethyl)furfural (HMF). Oligomerization and cross-condensation reaction of reactants and products are favored in the aqueous phase and can greatly hinder catalyst activity and selectivity to the desired products [8]. This

problem is especially serious for the catalytic upgrading of saccharides in an aqueous environment, since water facilitates the proton transfer reaction, thus increasing the formation of oligomerization products (humins) [8].

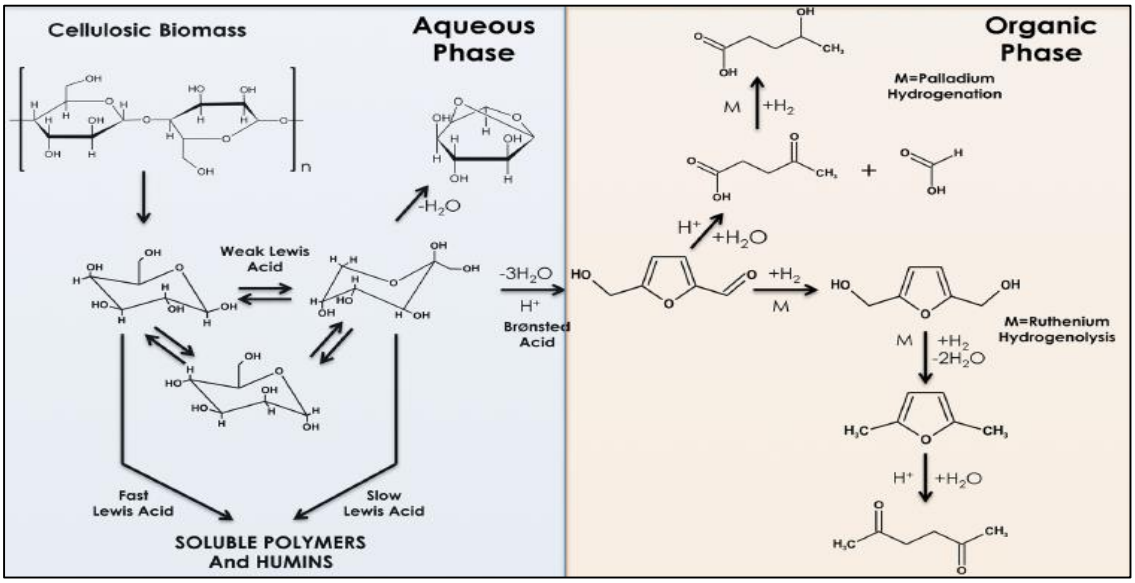

Figure 2: Reaction scheme for glucose conversion [8].

1.3.1 Glucose isomerization to fructose

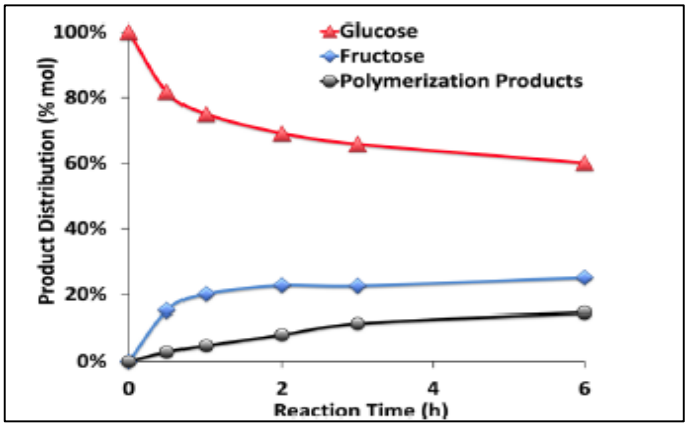

Figure 3: Product distribution for the isomerization reaction of glucose with time in the aqueous phase at 110° C, 600 rpm of agitation, and 400 psi of N_2 over NaX-MWNT nanohybrid catalyst (200 mg). The feed was 10 wt.% of glucose in a total reaction volume of 30 ml [8].

Figure 3, shows the product distribution for isomerization of glucose to fructose. At low conversion, the fructose selectivity was very high (e.g., around 85% when glucose

conversion <20%); however, after 2 h of reaction, the fructose yield reached a plateau while the glucose conversion kept increasing, as polymerization products were formed [8]. The observed additional disappearance of glucose can be ascribed to the heat-catalyzed degradation of saccharides toward soluble polymer and humins [8].

1.3.2 Glucose/Fructose dehydration

			product distribution (mol %)		
reactant	reaction time (min)	conversion (%)	5-hydroxymethylfurfural	formic acid	levulinic acid
glucose	30	34.4	1.4	5.0	5.5
	60	76.3	3.5	6.3	6.9
fructose	30	40.1	5.7	4.5	5.2
	60	65.5	31.5	8.2	8.6

[a]Reactant concentration: 10 vol % in 40 mL of total volume.

Figure 4: Conversion and Product Distribution obtained in the Dehydration Reaction of Glucose/Fructose at 150° C, 300 rpm of agitation and 600 psi of N_2 over 50 mg of nanohybrid catalyst (MWNT-SO_3H) in water/decalin (1/1 v/v)

Figure 4, shows the product distribution for dehydration reaction of glucose/fructose. It is seen that for glucose as feed and 30 min of reaction, the conversion achieved is 34.4% and 1.4 mol % of HMF is produced. With an increasing in time, conversion increases to 76.3%, but no appreciable increase in HMF mol% is observed, as there is an onset of the polymerization reaction. For fructose, with time conversion increases from 40.1% to 65.5%, which is reflected in the increase of HMF from 5.7% to 31.5%. The explanation for this behavior is, the stability of six-membered carbon ring of glucose is very high and hence, the open chain structure in solution are low. Contradictory to this fructose is unstable and has more open chain structure which is important for dehydration reaction. Also, fructose forms sterically hindered difructose dianhydrides that are sterically hindered, making cross polymerization less favorable than in the case of glucose [8].

1.3.3 Humin formation studies

Carl Lund et. al. has investigated the IR spectra of humins formed during the acid-catalyzed conversion of glucose, fructose, and 5-hydroxymethlfurfural. Figure 5 compares the IR spectra of humins formed from glucose, fructose, and HMF and it also

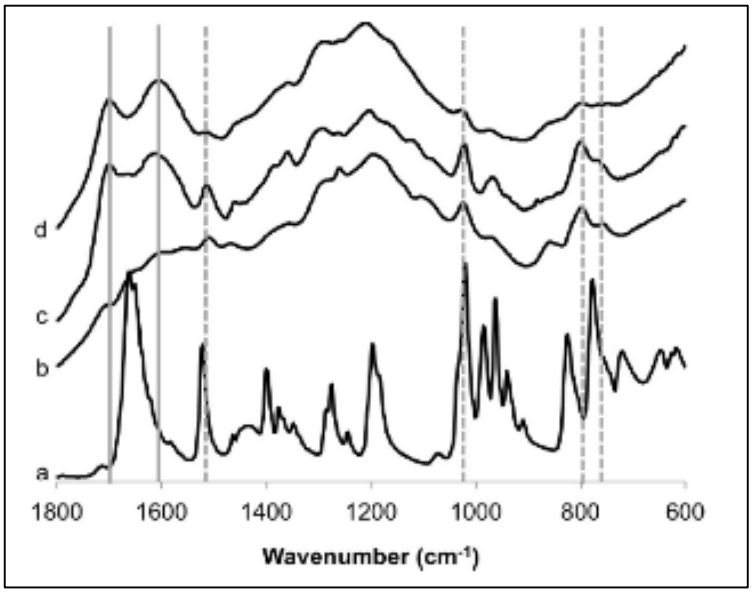

Figure 5: IR spectra of a) HMF and of humins formed using 0.1 M H_2SO_4 at 408 K from b) 0.1 M HMF at 90% conversion, c) 0.1 M fructose at 88% conversion, and d) 0.1 M glucose at 75% conversion [15].

shows the spectrum of HMF itself. The spectrum for all three reactants looked the same from 1100 cm^{-1} to 1400 cm^{-1} wavenumbers. There are two groups of spectral features where the intensities vary appreciable. The first group indicated in the figure by dashed gray lines include two peaks spanning from 750 cm^{-1} to 850 cm^{-1}, a peak at 1030 cm^{-1} and a peak at 1525 cm^{-1}. Considering that the peaks at 1030 cm^{-1} and 1525 cm^{-1} overlap with pure HMF peaks they concluded that it belongs to furan ring. The peaks at 750 to 850 cm^{-1} are shifted relative to HMF peaks, but they still considered them as arising from furan rings. DFT calculation of products of condensation of 2,5-dioxo-6-hydroxyhexanal (DHH) and HMF gave vibrational modes of furan ring in this range that do not appear at

the same frequencies as the corresponding modes in HMF [15]. Also, the intensities of all the peaks are much stronger in the case of fructose and HMF as compared to glucose. The second set of spectral features, two strong peaks at ca. 1625 and 1710 cm^{-1} indicated by solid gray line are prominent in the glucose and fructose humins while they cannot be distinguished in HMF humins. The location of these peaks is characteristic to carbonyl carbon group conjugated to an alkene group [15]. The intensities of these peaks helped to answer whether humins can directly be formed from glucose or fructose. In an aqueous environment, 90% of glucose and fructose exist as closed ring structure. Molecular dynamic simulation suggested that protonation of the hydroxyl group of glucose to be the rate determining step for its degradation at reaction condition used. Hence, humin formation via ether linkage does not seem likely. Also, with this mechanism, HMF could not polymerize but only dimerize, as HMF has only two hydroxyl groups. Adding to that, if etherification would be important for the formation of glucose humins one would expect the IR spectra of humins from HMF to differ from that of humins from glucose. In contrast to this hypothesis, the IR spectrum of glucose and HMF are quite similar in the range of 1050 cm^{-1} to 1300 cm^{-1}. Apart from the absence of an aldehyde group, sorbitol is similar in structure to glucose. Sorbitol is stable at similar reaction condition and does not form humins. Considering all these factors they concluded that aldehyde group is responsible for humin formation. Evaluating the aldol condensation/addition mechanism for humins formation via glucose aldehyde group, they were of opinion that it would result in two important consequences 1) the humin formed would have a single terminal carbonyl group 2) it would not be possible to incorporate side chain furan rings. They conducted few experiment of humins formed from glucose/fructose and

benzaldehyde. The IR spectrum of humins after reaction showed the presence of benzene ring in humins. The experimental results were completely opposite to the hypothesis mentioned earlier and hence they were of the conclusion that humins are not formed from glucose and fructose directly. Another possibility they considered is glucose and fructose

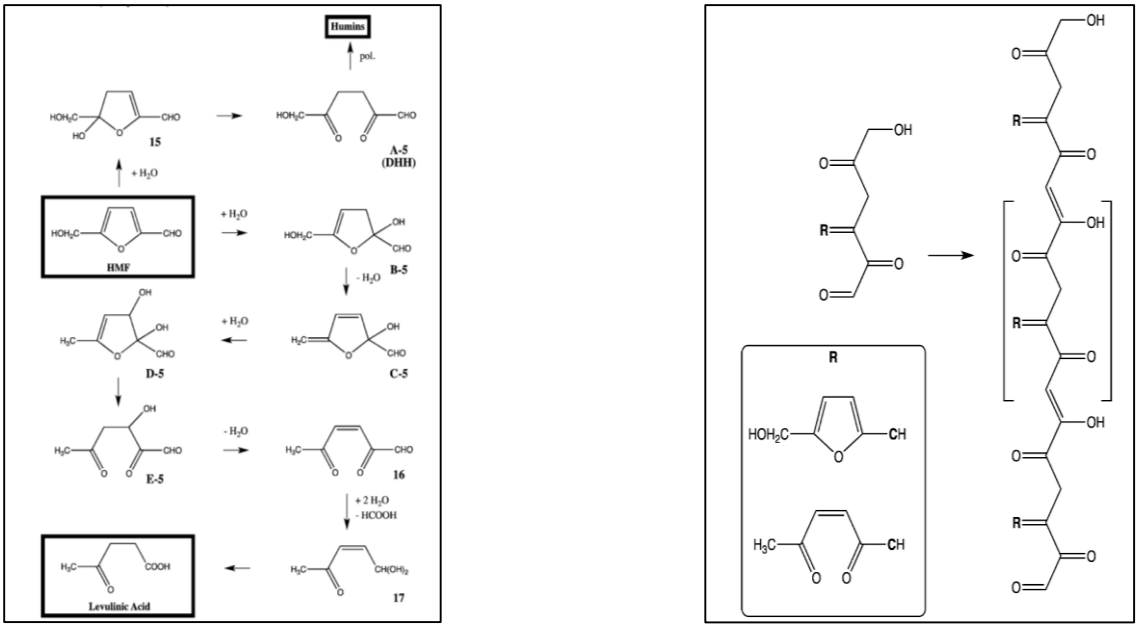

Figure 6: On left, Horvat mechanism for HMF conversion and on right, idealized Humin structure

are converted to HMF and further HMF undergoes acid hydrolysis in the presence of water to form DHH, which is primarily responsible for humins formation. If this was true the IR spectra for all three reactants would be same, which is not the case. Hence, the difference in spectra can be attributed to aldehyde and ketone group reacting with DHH. That is all the three spectra have the same backbone of DHH while the side groups would differ. In the case of humin formation from HMF, initially concentration of HMF is quite high and hence, the side group with furan ring reacts with DHH, which explains the high-intensity peaks of furan ring in humins from HMF. Gibbs free energy calculation also advocates the same thing. But it raises the question of why peaks at 1625 cm^{-1} and 1710

cm^{-1} are not present in humins formed from HMF. The explanation for this is, assuming the humin structure is formed as shown on the right-hand side of figure 6. On close observation, we see that furan rings and hydroxyl groups are also in conjugation with a double bond. The conjugated carbon-carbon vibration in furan ring and the vibration of the hydroxyl group are expected to couple with those of the carbon-carbon double bonds conjugated to carbon-oxygen double bonds. In the case of glucose, HMF is not present in appreciable quantity and hence the compound indicated as 16 in figure 6 reacts with DHH. This explains why the peaks at 1625 cm^{-1} and 1710 cm^{-1} are predominant in the case of glucose. When fructose is used as feed initially HMF is in low concentration and hence compound 16 reacts with DHH giving peaks at 1625 cm^{-1} and 1710 cm^{-1}, as the reaction proceeds concentration of HMF increases and side groups with furan rings dominate. Hence, the strong intensity of both groups of spectral features in fructose humins can be explained by a postulate that they are produced via aldol addition/condensation polymerization of DHH [15].

1.3.4 Biphasic Reaction System

The issue of humin formation can be avoided by the use of biphasic system. With

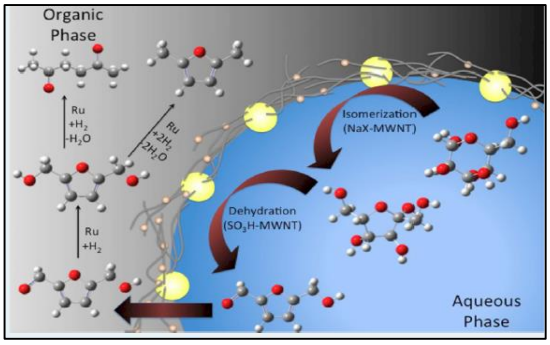

Figure 7: Schematic representation of glucose conversion in a biphasic system [8]

the help of this system, reaction and separation can be simultaneously accomplished by

taking advantage of differences in solubility of reactants and products [8]. It consists of an organic phase and aqueous phase. For glucose isomerization/dehydration reaction the most common biphasic system used is THF/Water (35 wt% salt). As we know THF is soluble in water, saturating water with salt helps in creating a different phase. Salt also helps in separating HMF formed from the aqueous phase. Feed glucose, is present in the aqueous phase. Adding hydrophobic catalyst to this system and sonicating for 30 min under horn sonicator produces a stabilized emulsion, with the catalyst at interface. Depending on the degree of functionalization of catalyst we can obtain water in oil or oil in water emulsion. Glucose diffuses to the interface where it isomerizes/dehydrates to HMF. HMF formed is then transferred to the organic phase, where further upgrading of HMF takes place. Avoiding the contact of HMF with water suppresses the formation of DHH which in turn reduces humin formation. This hypothesis is proved experimentally in next section.

1.3.5 Glucose isomerization/dehydration to HMF in single phase and biphasic system

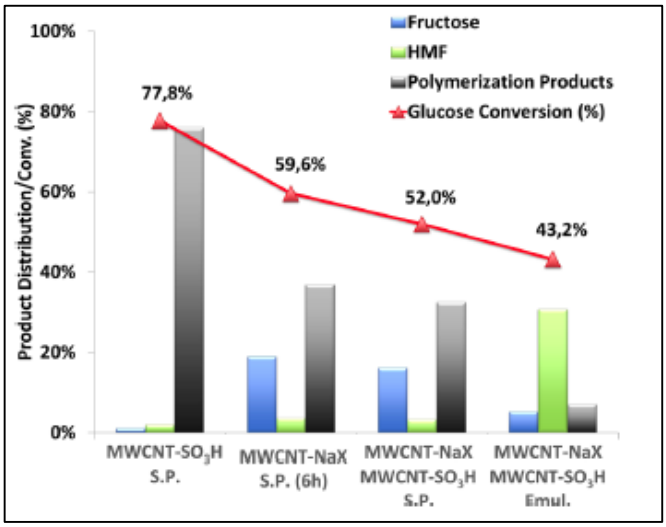

Figure 8: Conversion of glucose and product distribution from the isomerization/dehydration reaction in single phase (S.P.) and in water (35 wt% NaCl)/THF emulsion of glucose (Emul.). Reaction were carried out at 150° C, 600 rpm of agitation, and 400 psi of N_2 [8]

As shown in figure 8, in the presence of MWCNT-SO_3H in a single phase (water), all of the glucose converted goes to polymer products. The reason for this is same as mentioned earlier, the stability of glucose is higher and hence open chain compounds are less. Also, the presence of bronsted acid catalyst makes it easier for protonation of hydroxyl groups resulting in polymer products. MWCNT-NaX in a single phase (water) gives ca. 19% of fructose and ca. 40% of polymer products. Lewis acid catalyst MWCNT-NaX isomerizes glucose to fructose but as we don't have a bronsted acid catalyst to further convert fructose to HMF, heat catalyzed degradation of saccharides to soluble polymer and humins takes place [8]. When MWCNT-NaX (lewis acid) and MWCNT-SO_3H (bronsted acid) catalyst are present in a single phase (water), the conversion is 52% and polymerization products are ca. 30%. More than half of the glucose converted goes to polymer products. Due to single phase (water) the HMF formed cannot be separated and hence undergoes humins formation mechanism. On contrary when we have biphasic

reaction system (emul.) an appreciable increase in HMF concentration is noticed. As stated earlier, as we separate HMF from the aqueous phase, DHH formation is suppressed and hence, humin formation is also reduced. HMF can further be upgraded in the organic phase.

1.4. 5-(hydroxymethyl) furfural up gradation

Once HMF is transferred to organic phase it can further be upgraded by hydrogenation/hydrogenolysis. The products produced by hydrogenation of biomass derived 5-(hydroxymethyl) furfural are a potential substitute for petroleum-based building blocks used in the production of chemicals [16]. HMF serves as a good monomer for polymer industry because of its hydroxyl, aldehyde functionalities, and a furan ring. HMF is converted to 2,5-furandicarboxylic acid which is a potential alternative to terephthalic acid [17]. Aldol condensation of HMF with acetone followed by hydrogenation and hydrogenolysis yields jet fuel [18]. Depending on the type of metal/acid catalyst we choose we can change the selectivity towards one particular

			product distribution (mol %)		
catalyst	HMF conversion (%)	TOF (s^{-1})	2,5-bis(hydroxymethyl) furan	2,5-hexanedione	γ-hydroxyvaleric acid
5% Ru/MWNT/Al_2O_3	70.7	0.25	15.0	47.8	7.8
5% Pd/MWNT/Al_2O_3	87.0	0.34	2.9	0	84.1

[a]Feed: 1 g of hydroxymethylfurfural in 40 mL of total volume.

Figure 9: Conversion of Hydroxymethylfurfural (HMF) and product distribution obtained in the Hydrogenation Reaction of HMF after 2 h of Reaction at 150° C, 300 rpm of agitation, and 600 psi of N_2 over 50 mg of Nanohybrid Catalyst (5% Ru/MWNT/Al_2O_3 and 5% Pd/MWNT /Al_2O_3) in water decalin (1/1) Emulsion [8]

product. Reaction scheme for HMF up gradation is shown in Figure 1. HMF is hydrogenated to 2,5 bis(hydroxymethyl) furan (BHF) which on hydrodeoxygenation yields 2,5 dimethylfuran (DMF). DMF on ring hydrogenolysis produces 2,5 hexanedione

(HXD). BHF and HXD are potential monomers for polymer industry. HMF on ring hydrogenolysis yields levulinic acid and formic acid. Levulinic acid is hydrogenated to γ-hydroxy valeric acid. Dehydration of γ-hydroxy valeric acid gives γ-valerolactone, which is a potential green solvent [19]. As shown in figure 9, Ru/MWNT/Al_2O_3 is a bifunctional catalyst, where Ru provides hydrogenation functionality and Al_2O_3 provides lewis acidity for ring hydrolysis. Ru catalyst is selective towards 2,5-hexandione and Pd catalyst produces γ-hydroxy valeric acid as the major product. As Ru has more hydrogenation capabilities, the C-O bond of HMF is readily hydrogenated forming BHF and the end product is HXD. Pd has lower hydrogenating capabilities and hence lewis acidity dominates. As a result, HMF is first ring hydrolysed to Levulinic acid and formic acid. Hydrogenation of levullinic acid yields γ-hydroxy valeric acid. Acid metal balance is a subject of further study.

1.4.1 HMF to 2,5 Dimethylfuran

property	DMF	gasoline	bioethanol
molecular formula	C_6H_8O	C_4–C_{12}	C_2H_6O
molecular mass (g/mol)	96.13	100–105	46.07
liquid density (kg/m^3, 20 °C)	889.7	744.6	790.9
relative vapor density	3.31	3–4	1.59
latent heat of vaporization (kJ/mol, 20 °C)	31.91	38.51	43.25
energy density (MJ/L)	31.5	35	23
boiling point (101 KPa)	92–94	96.3	78.4
water solubility (25 °C)	immiscible	immiscible	miscible
research octane number	119	95.8	110

Figure 10: Comparison of DMF, Gasoline and bioethanol [3]

DMF is considered as a new-fashioned liquid biofuel for transportation. Compared to current market leading bioethanol, DMF possesses higher energy density (31.5 MJ/L), higher boiling point (92-94° C), and a higher octane no. and is not soluble in water [20]. Also, as shown in figure 10, DMF is more similar in properties to gasoline as compared to bioethanol [3]. Hydrogenation/hydrodeoxygenation of HMF over Ru/C to DMF was investigated by Shijie Liu et al. They optimized the conditions such as temperature, time, catalyst loading, H_2 pressure, HMF concentration and agitation speed with THF as a solvent. Maximum HMF conversion and DMF yield achieved were 100% and 94.8% respectively for reaction parameters of 200° C, 2 hrs, 5 mol% Ru/C (with

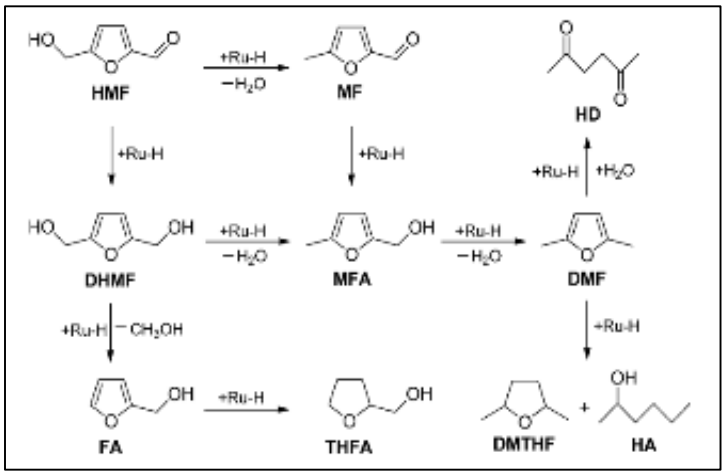

Figure 11: Plausible Mechanism for the hydrogenation of HMF into DMF over Ru/C [17].

respect to HMF), 290 psi H_2 pressure, 2.5 wt% HMF and 400 rpm of agitation speed [20]. Similar reaction conditions and solvent system is used for carrying out experiments with HMF hydrogenation. They also observed other compounds in the reaction mixture and hence they suggested a plausible mechanism (figure 11). Hydrogen activated Ru can hydrogenate and dehydrate hydroxyl group of HMF forming 5-methyl furfural (MF). It can also hydrogenate C=O bond forming 2,5-bis(hydroxymethyl) furan (BHF). MF and

BHF are hydrogenated to DMF via intermediate methyl furfuryl alcohol (MFA). They also tested for reusability of Ru/C. Catalyst can be recycled 3 times without any significant loss of activity. After 5 cycles they observed Ru leaching and agglomeration of the carbon support, thus decreasing Ru sites and surface area. Regenerating catalyst restores its activity. In another approach, Pt/AC (activated carbon) and Pt/GC (graphitized carbon) for HMF hydrogenation were compared. DMF yield of 9% and 56% were obtained, respectively [20]. When the two catalysts were modified with Cobalt to form PtCo/AC and PtCo/GC, HMF conversion of 100% and DMF yield of 98% were obtained. Hence, they concluded that alloy is crucial for selective hydrogenation of HMF to DMF.

1.4.2 HMF to cyclopentanone derivatives

Cyclic ketones, particularly cyclopentanone derivatives are an important reactant for aldol condensation reaction which yields diesel range products [21]. Ring rearrangement

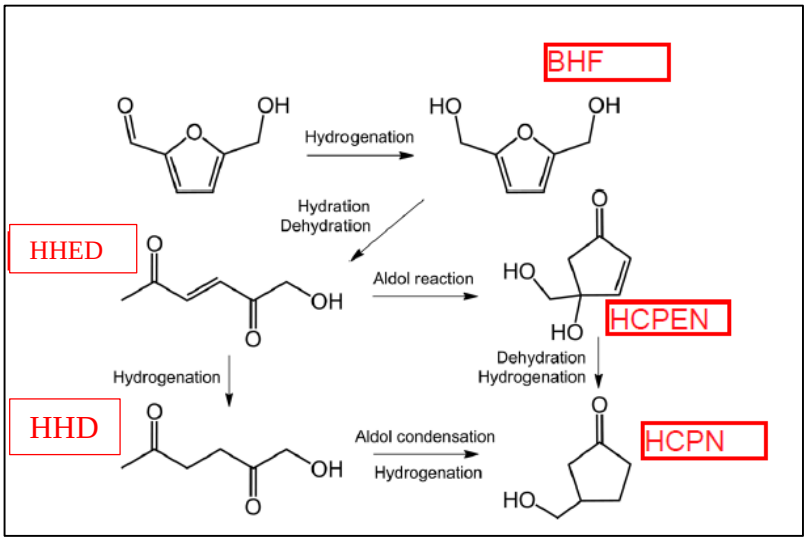

Figure 12: Hydrogenation and ring rearrangement of HMF to HCPN [22]. HHED: 1-hydroxy-3-hexene-2,5-dione; HHD: 1-hydroxy-2,5-hexanedione; BHF: 2,5-bishydroxymethylfuran; HCPEN: 4-hydroxy-4-hydroxymethyl-2-cyclopentenone; HCPN: 3-hydroxymethylcyclopentanone.

reaction of HMF to cyclopentanone derivative by selective hydrogenation on Au nanoparticles and the Lewis acid catalyst of metal oxide supports, was studied by Atsushi

Satsuma et. al. Au is known for selective hydrogenation of unsaturated aldehydes [22]. Acidic and basic supports were compared for ring rearrangement products. Acidic supports gave higher yields of ring rearrangement products as compared to basic supports. Maximum conversion of HMF, >99% and 3-hydroxymethylcyclopentanone yield of 86% was observed for Au/Nb_2O_5. Based on yield vs time plot for HMF hydrogenation over Au/Nb_2O_5, they proposed reaction scheme shown in figure 12. The selective hydrogenation over Au gives 2,5 bis(hydroxymethyl) furan (BHF). BHF on acid sites undergoes ring opening to 1-hydroxy-3-hexene-2,5-dione (HHED). Hydrogenation of HHED produces 1-hydroxyl-2,5-hexanedione (HHD) which on intramolecular aldol condensation followed by hydrogenation yields 3-hydroxymethylcyclopentanone (HCPN). Also intramolecular aldol condensation of HHED gives 4-hydroxy-4-hydroxymethyl-2-cyclopentenone (HCPEN). HCPEN on dehydration and hydrogenation gives HCPN. The acidity of support first works for the ring opening reaction, and then for aldol condensation and dehydration reactions. Au particle size for different samples was analyzed by X-ray absorption fine-structure spectral analysis. They concluded that Au particle size did not have an effect on the yield of HCPN. Analyzing Fourier transform infrared spectroscopy of pyridine adsorbed on different support they came to the conclusion that lewis acid sites on Nb_2O_5 are responsible for ring opening of BHF.

1.5 Furfural up grading

Electricity generated from various renewable resources such as wind and solar power can be utilized for transportation, organic chemicals cannot be produced from most renewable resources except biomass. Therefore, development of the production systems of chemicals, especially monomers for plastics with large demands, is critically important for sustainable society [23]. Furfural is one compound with proper no. of carbon and

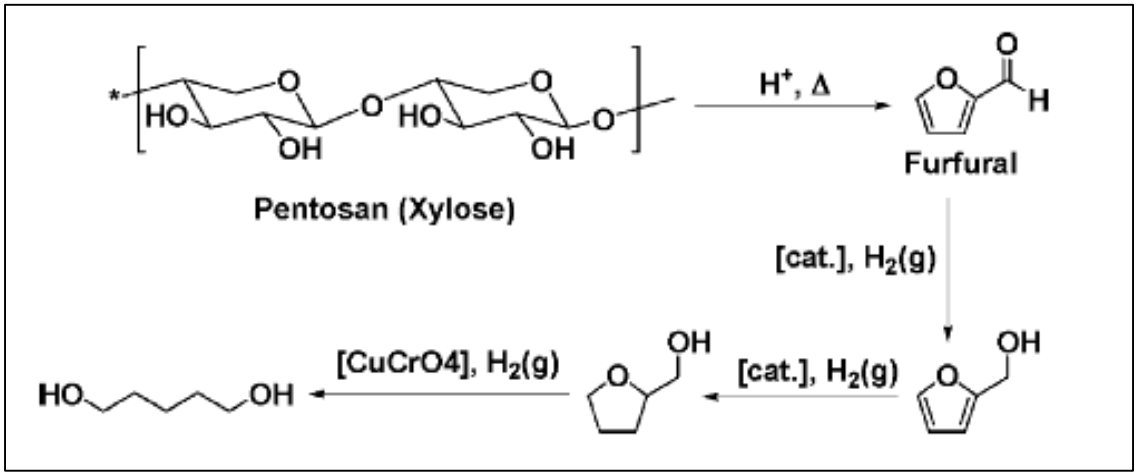

Figure 13: Pathway for conversion of hemicellulose (xylose) to 1,5-pentanediol [27]

oxygen atoms. It can be upgraded to 1,5-pentanediol which has numerous application as plasticizer and in pharmaceutical industry.

Hemicellulose accounts for 28% to 55% of biomass [5]. Xylans forms a major portion of hemicellulose [24]. Acid hydrolysis of xylans produces xylose. Xylose is isomerized to xylulose over Sn-beta zeolite. A conversion of 60 %, with 27% yield of xylulose is obtained at 100° C [24]. Xylulose is dehydrated to furfural over amberlyst-15, with 66% conversion and 27% yield of furfural [24]. Furfural is hydrogenated to Tetrahydro furfuryl alcohol (THFAL) over Cu/Ni bimetallic catalyst. A 100% conversion of furfural, with 98% yield of THFAL is achieved [25]. THFAL can be converted to 1,5-pentanediol by two different methods. THFAL on direct hydrogenolysis yields 1,5-

pentanediol, 1,2-pentanediol and methyl tetrahydrofuran depending on position of C-O bond scission. A maximum 85% yield of 1,5-pentanediol on Rh-MoO_x/SiO2 (Mo/Rh =

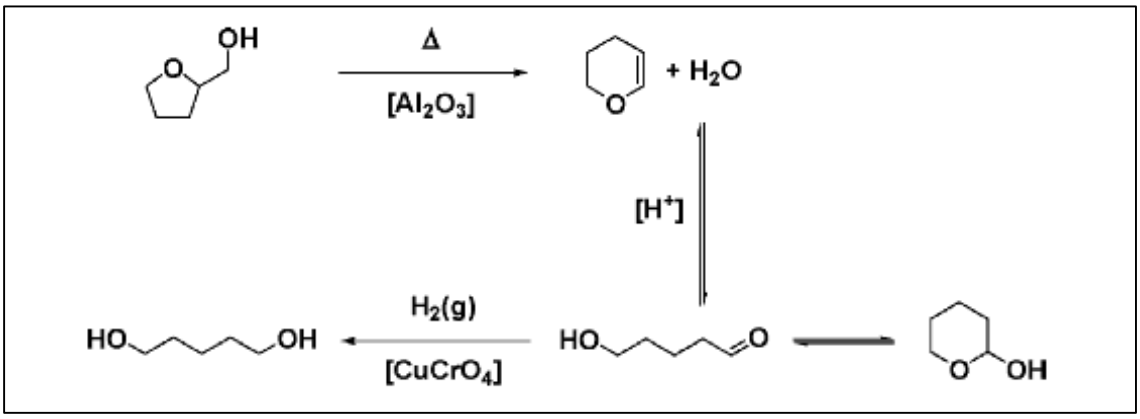

Figure 14: Multi-step process for transformation of tetrahydrofurfuryl alcohol to 1,5-pentanediol [26].

0.13) was attained in 24 hrs, with 94.2% conversion of THFAL [10]. The disadvantage with direct hydrogenolysis is, it produces 1,2-pentanediol as byproduct, expensive catalyst requirement i.e. Rh-MoO_x/SiO_2, high H_2 pressure and longer reaction time is required. The multi-step process involves dihydropyran and δ-hydroxyvaleraldehyde as intermediate in THFAL conversion to 1,5-pentanediol, achieving 70% overall yield of 1,5-pentanediol [26]. But, multi-step process requires isolation and purification of intermediates by distillation in order to achieve high yield of products [27]. 87% yield of 3,4 dihydropyran is achieved when THFAL is treated with activated alumina at 375° C in a gas reactor [28] [29]. Treating 3,4 dihydropyran with 0.2 N hydrochloric acid for 40 minutes resulted in 78.2% yield of δ-hydroxyvaleraldehyde [28]. In a bomb reactor δ-hydroxyvaleraldehyde was treated with copper chromite for 15 min, at 2000 psi H_2 pressure and 150° C temperature [28]. 96.2% yield of 1,5-pentanediol was achieved. The combined yield of all the three steps was 70% [28].

Chapter 2: Experiment

2.1 Catalyst Preparation

2.1.1 5 wt% Pd/MWCNT

It was prepared by incipient wetness impregnation method. Palladium (II) nitrate dihydrate (~40% Pd basis, Sigma-Aldrich) salt was used for impregnation on black sand MWCNT, procured from SouthWest NanoTechnologies Inc. After drying the impregnated catalyst overnight in oven at 100° C, it was calcined in air at 300° C for 3 hrs.

2.1.2 2 wt% Ru/TiO_2

It was prepared by incipient wetness impregnation method. Ruthenium (III) nitrosyl nitrate solution (in dilute nitric acid, Sigma-Aldrich) salt was impregnated onto Titanium (IV) oxide (>99.5% trace metal basis, P25, Sigma Aldrich). The catalyst was dried overnight at 100° C for 12 hr. It was then calcined in air at 400° C for 4 hr.

2.1.3 5 wt% Cu/SiO_2-Al_2O_3

SiO_2-Al_2O_3 grade 135 (SiO_2/Al_2O_3 = 5.8, pore volume = 0.76 ml/g, surface area = 475 m^2/g) was used as support. Cu was impregnated by wetness impregnation method. Required amount of $Cu(NO_3)_2$ 2.5 H2O was dissolved in a 0.1M solution of ammonium nitrate and added to the silica alumina catalyst support according to its pore volume. The catalyst was dried at 120° C for two hours and calcined at 500° C for 4 hours [30].

2.1.4 MCM-41-SO_3H-PTS (1:1)

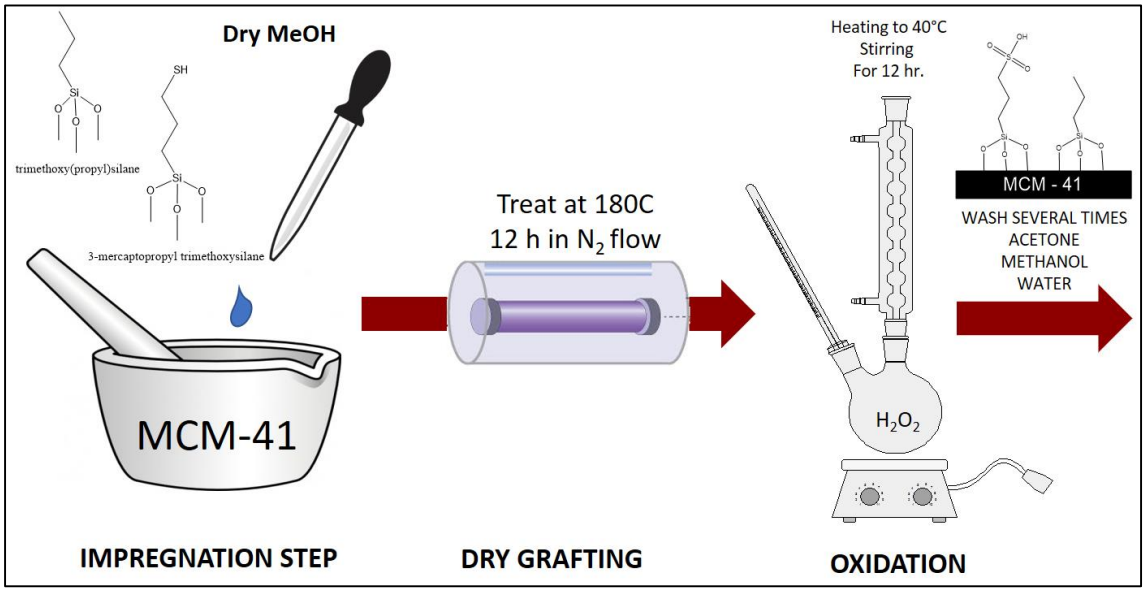

Figure 15: Schematic diagram of MCM-41-SO_3H-PTS preparation method

Functionalization of MCM-41 is carried out by incipient wetness impregnation method, dry grafting and oxidation. Trimethoxy(propyl)silane (PTS) and 3-mercaptopropyl trimethoxysilane (MPTMS) are mixed in required ratios in dry methanol. Dry methanol is added as per the pore volume of MCM-41 i.e. 0.63 ml/g of MCM-41. The reason for using dry methanol is, the water present in methanol might carryout hydrolysis of silane groups. The solution is added drop wise to MCM-41 and mixed using a mortar and pastel. The impregnated MCM-41 is then dry grafted in a calcination tube at 180° C for 12 hrs. in flow of N_2. After calcination, oxidation of -SH group is carried out in hydrogen peroxide at 40° C with constant stirring for 12 hrs. MCM-41-SO_3H-PTS is then filtered and washed with acetone, methanol and water several times. SO_3H group is hydrophilic and trimethoxy(propyl)silane is hydrophobic. Hence, we can tune the hydrophobicity of the catalyst by changing the ratio of PTS to MPTMS. The catalyst is found to be stable in organic solvent up to a temperature of 350° C. The IR results of

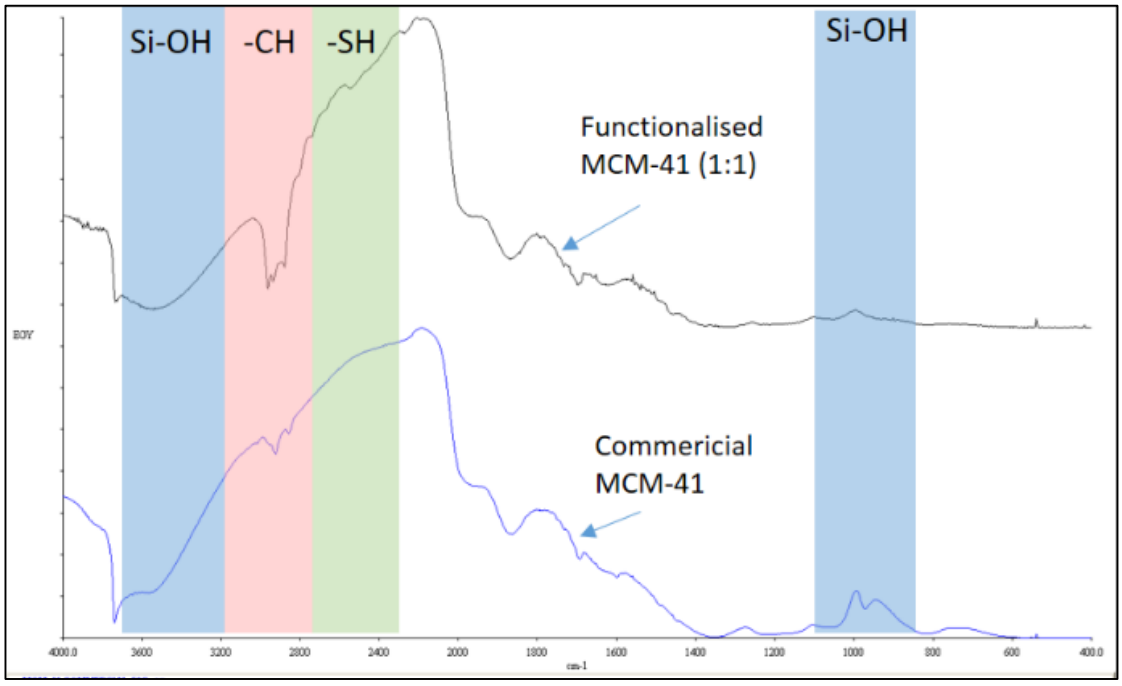

Figure 16: IR spectroscopy results of commercial MCM-41 and MCM-41-SO_3H-PTS (1:1)

*Work done by Santiago Umbarila

commercial MCM-41 and MCM-41-SO_3H-PTS (1:1) are shown in figure 16. The wavenumber from 3200 cm^{-1} to 3600 cm^{-1} and 800 to 1100 cm^{-1} represents silanol groups of MCM-41, 2800 to 3200 cm^{-1} represents -CH interaction from propyl chain and 2300 to 2700 cm^{-1} represents mercaptan groups. We see a drop in silanol group intensity for functionalized MCM-41-SO_3H-PTS (1:1), indicating functionalization of catalyst has taken place.

2.2 Experimental set up

2.2.1 Glucose Upgrading

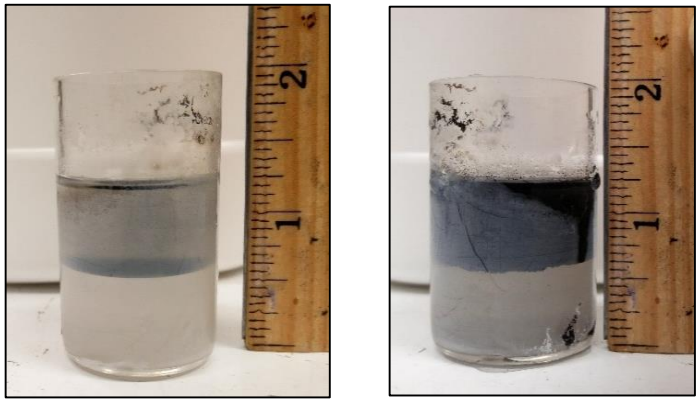

Figure 17: Image of reaction mixture before (left) and after (right) sonication

Glucose upgrading reactions were carried out in a 50 ml Parr batch reactor, equipped with Parr 4843 Temperature controller. Tetrahydrofuran (anhydrous 99.9%, inhibitor free, Sigma Aldrich) was used as organic phase. De-ionized water with 35 wt.% salt (NaCl, 99.6%, JT Baker) was used as aqueous phase. 10ml salt solution (35 wt.% NaCl salt) was taken in a glass liner that perfectly fits in the bottom vessel of the reactor.

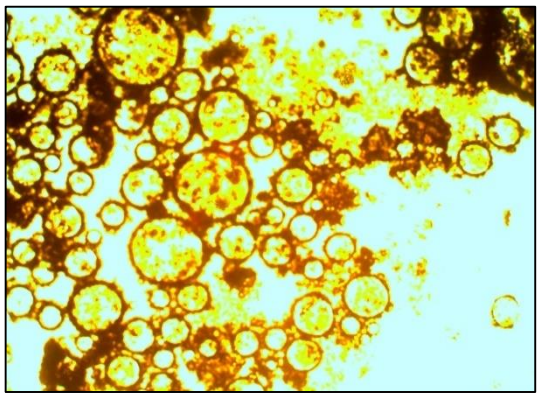

Figure 18: Optical microscope image of interface

To that was added α-D-glucose (anhydrous 96%, Sigma - Aldrich) or D-fructose (Sigma-Aldrich) by 5 wt% (of solvent and feed). 10 mg of 5wt% Pd/MWCNT was added. Finally, 10 ml THF was added. The reaction mixture appeared as shown in figure 17, on left, with

top layer as THF, bottom layer as D.I. water and catalyst sits at the interface. The reaction mixture was then sonicated with horn sonicator for 30 min with 25% amplitude. As MWCNT are hydrophobic, sonication leads to the formation of water in oil emulsion. The reaction mixture is then checked under an optical microscope to look for droplets of water being formed and stabilized by MWCNT (Figure 18). This ensures that emulsion has been formed. The glass liner was then placed inside the reactor bottom vessel. The reactor was then sealed and connected to reactor assembly. The reactor was purged with N_2 for the first time. Then the gas was changed to H_2, reactor was purged twice and checked for leaks. It was pressurized with 800 psi of H_2 at room temperature and stirring speed was set at 500 rpm. The heater was turned on. The pressure inside the reactor increased to 1000 psi and reaction was carried out for 2 hrs. At the end of 2 hrs. the reactor was cooled to room temperature quickly by quenching the bottom vessel of reactor in an ice bath. The reaction mixture was transferred to a glass vial and centrifuged so that catalyst settles at the bottom of the organic phase. The two phases were separated using a separating funnel. Both the phases were filtered using a 0.2 µm PTFE syringe filter. The organic phase was analyzed by GC-MS for peak identification and in GC-FID for quantitative analysis. The aqueous phase was analyzed by HPLC. The sample was diluted 3 times with water due to the presence of salt in the aqueous phase which may damage HPLC column.

2.2.2 HMF Upgrading

Decalin (anhydrous, >99%, Sigma Aldrich) as solvent and THF as co-solvent are used for HMF upgrading reactions. We use Decalin, as THF has a higher vapor pressure. THF is used, as HMF is insoluble in Decalin. 50 ml Parr batch reactor, equipped with Parr

4843 temperature controller was used for carrying out reactions. 20 ml decalin and 50-100 mg of Ru/TiO_2 catalyst is loaded into reactor bottom vessel. The reactor is sealed and reduction of catalyst at 250° C, 500 psi pressure is carried out for 2 hrs. After reduction, reactor temperature is set to 220° C and reactor pressure is set to 200 psi. Feed i.e 0.41g HMF, dissolved in 15 ml THF is injected to feed cylinder using a 20 ml glass syringe. The feed cylinder is then pressurized to 600 psi of H_2. The feed is then injected into the reactor by opening the feed valve. The final pressure and temperature inside the reactor reaches 550 psi and 200° C. The reaction is carried out for 2 hrs. At the end of 2 hrs. the reactor is quenched in an ice bath. The reaction mixture is filtered with 0.2 µm PTFE membrane syringe filter to separate catalyst particle. 10 µL of internal standard i.e 1,4 dioxane is added to 10 ml of reaction sample. Internal standard is used to eliminate the error caused due to inconsistency in the injection of sample in GC-FID. This mixture is then injected in GC-FID and GC-MS for quantitative analysis and peak identification. Response factor for each component is determined by plotting a graph of the ratio of the concentration of component standard to the concentration of internal standard on y-axis and ratio of Area of component Standard from GC-FID to Area of the internal standard from GC-FID on the x-axis. The slope of this graph is response factor. Using this response factor, the area from GC-FID for respective component and area of Internal standard the yield for each component is calculated.

2.2.3 Furfural Upgrading

50 ml Parr batch reactor equipped with Parr 4843 temperature controller was used for carrying out furfural upgrading reactions. For reaction with Cu/SiO_2-Al_2O_3, the reduction of catalyst is carried out in solvent free condition. The advantage of using

solvent free condition is, there is no mass transfer limitation for hydrogen to diffuse into the solvent. Also in many cases solvent reacts with catalyst during reduction. Catalyst was first loaded into reactor bottom vessel. The reactor was sealed, fitted into the reactor assembly and purged with nitrogen and hydrogen. While purging, caution has to be maintained, so that catalyst is not carried out of the reactor along with purge gas. Reactor is heated to 300° C and reduction of catalyst is carried out for 4 hrs. [30]. After the reduction, reactor is cooled to room temperature. Solvent and feed are introduced via feed cylinder. Reactor is heated to reaction temperature and reaction is carried out for desired reaction time. Time zero is the point when reactor temperature reaches desired reaction temperature. At the end of reaction, reactor is cooled in an ice bath to room temperature. The volume of reaction mixture is measured and transferred to a glass vial. Reaction mixture is filtered using PTFE 0.22 µm syringe filter. 1 ml of 1-propanol (Sigma-Aldrich, 99.7%) as internal standard is mixed with 1 ml reaction mixture. 1-propanol also helps in dissolving any insoluble products. This solution is analyzed in GC-MS (ZB-1701 column) for peak identification. Quantitative analysis is carried out in GC-FID equipped with ZB-WAXPLUS (60m x 250 µm x 0.25 µm) column. The yield of products and conversion is calculated by using calibration curves and area of product from FID. The formulas used for calculation are similar to the ones mentioned in section 2.5.

2.3 Peak identification and quantitative analysis

For peak identification, Shimadzu GCMS-QP 2010S is used. It is equipped with ZB-1701 column (60m x 0.25mm x 0.25µm). Separation is based on polarity and molecular weight basis. The carrier gas is helium. Injection temperature is 275° C.

Aqueous phase is analyzed by HPLC with UV and IR detectors. The column used is Aminex HPX87C (separation based on polarity). 5mM H_2SO_4 is used as the mobile phase.

Quantitative analysis is carried out in GC-FID with ZB 1701 column. Separation is based on mid-polarity.

2.4 Calibration curve

All the identified peaks were calibrated using standards. To account for error in injection in GC-FID, calibration was done with respect to an Internal standard. The ratio of the concentration of standard compound to the concentration of Internal standard was plotted on the y-axis. The ratio of Area of standard compound from GC-FID to the area of the internal standard from GC-FID was plotted on the x-axis. The slope of the graph is known as response factor. Calibration curves for few of the compounds are shown below. Calibration curve for all the other compounds are shown in Appendix A.

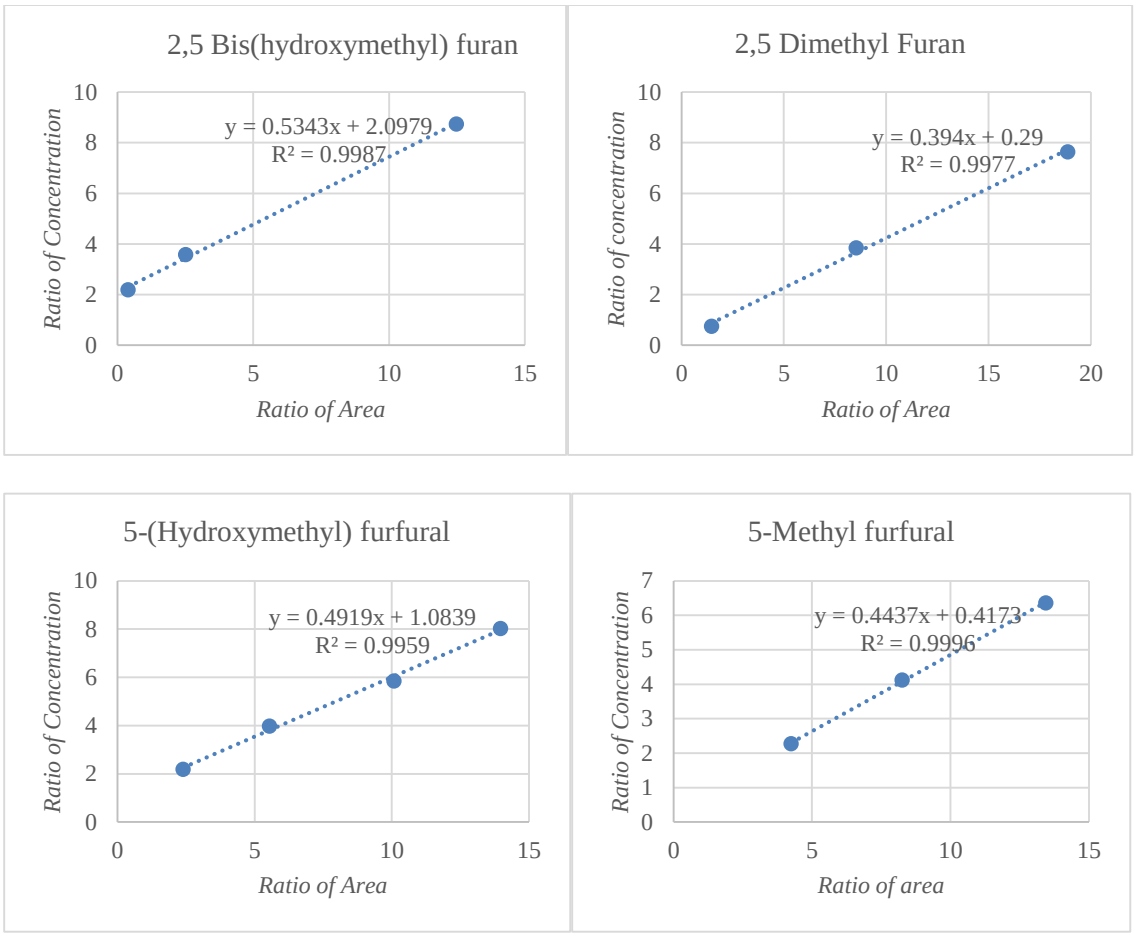

Figure 19: Calibration curves

2.5 Calculations

The concentration of a particular product or reactant is found using response factor, the area of product from GC-FID, area of the internal standard from GC-FID and concentration of the internal standard. Yield, selectivity, carbon balance and conversion are calculated as shown below. The moles of reactant initially refer to moles of feed at time t = 0 which is calculated by doing a blank injection. This accounts for losses of feed during injection.

$$Conversion = \frac{moles\ of\ reactant\ initially - moles\ of\ reactant\ finally}{moles\ of\ reactant\ initially} \times 100$$

$$yield\% = \frac{moles\ of\ product}{moles\ of\ reactant\ initially} \times 100$$

$$Selectivity\% = \frac{moles\ of\ product\ A}{Total\ moles\ of\ prodcut} \times 100$$

$$Carbon\ balance = \frac{moles\ of\ product + moles\ of\ reactant\ finally}{moles\ of\ reactant\ initially} \times 100$$

$$Mole\ balance = \frac{moles\ of\ product}{moles\ of\ reactant\ reacted} \times 100$$

Chapter 3: Experimental Results

3.1 Glucose upgrading

A typical GC-FID chromatogram of organic phase for glucose as feed, with 5 wt% Pd/MWCNT as catalyst is shown in figure 20. The yield of ketones combined is quite high as compared to other products. The products marked by green circle are identified by GC-MS and by standard injection. The remaining peaks are yet to be identified. The compound shown for unidentified peaks are predicted by GC-MS library with low % of mass spectrum match. Ketones are a good alternative to petroleum-based monomers used in polymer industries. 2,5-hexanedione is formed by ring hydrogenolysis of 2,5 dimethyl furan. The residual acidity on MWCNT may be responsible for carrying out ring hydrogenolysis. 2,5-hexanedione can undergo self-aldol condensation to form 2-methylcyclopentanone and 3-methylcyclopentanone [31]. Cyclic ketones can further undergo aldol condensation reaction to form diesel range products.

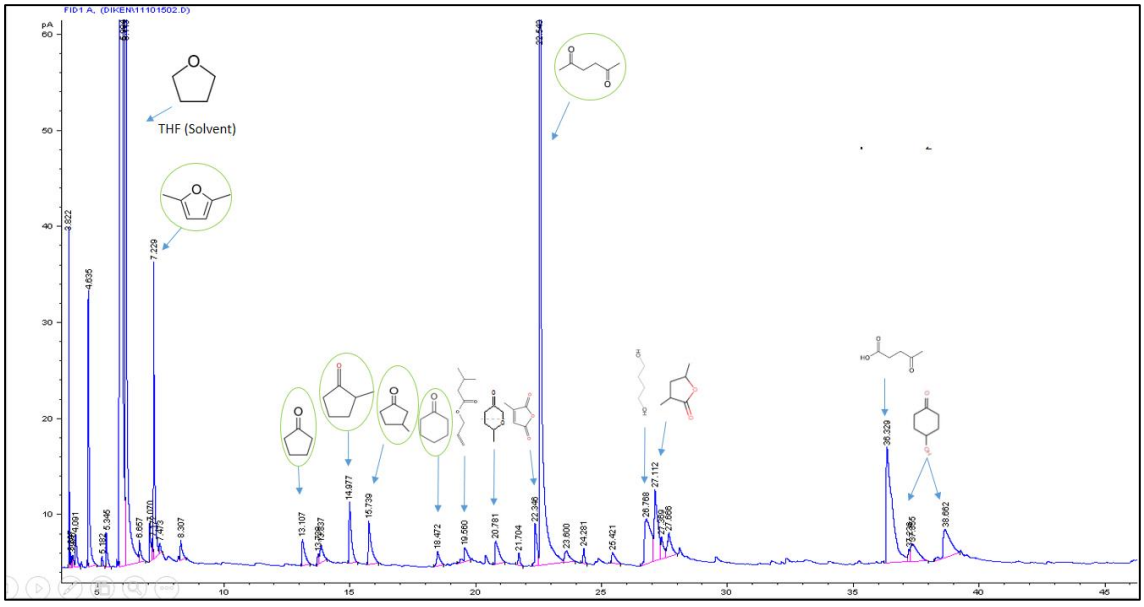

Figure 20: GC-FID chromatogram for feed 5 wt% glucose, 10 mg 5 wt% Pd/MWCNT, Temp. 200° C, pressure 1200 psi H_2 and 2 hrs. of reaction time.

3.1.1 Temperature variation

As seen in Table 1, by increasing the temperature from 200° C to 250° C there is an increase in mole balance from 27.64% to 40.69%. The explanation for this is the possibility of furans being adsorbed to carbon nanotubes as it is shown by Daniel Resasco et al. that activated charcoal is used for filtration of furanics and phenolics [13]. As we increase the temperature, furanics and other compounds start desorbing from MWCNT. Results from further increasing the temperature are shown in table 9 of Appendix A. Mole balance is calculated as defined in section 2.5.

Temp. (C)	**Yield %**							**Mole balance**
	2,5 DMF	2,5 HXD	N-butyl methyl ketone	CPT	2-methyl CPT	3-methyl CPT	CHX	
200	2.76	10.27	0	0.58	0.89	0.84	0.28	27.64
250	5.65	14.87	2.87	2.04	2.59	1.92	2.20	40.69

Table 1: Temperature variation for reaction with 5 wt% glucose as feed, 10 mg 5 wt.% Pd/MWCNT, pressure (1500 psi H_2), reaction time (2 hrs.). The conversion for both reactions is 100%. DMF: Dimethyl furan; HXD: hexanedione; CPT: cyclopentanone; CHX: cyclohexanone.

3.1.2 Time variation

With the increase in time, there is an increase in mole balance. These data again point out to molecules being desorbed from carbon surface.

Time (hrs)	**Yield %**						**Mole balance**
	2,5 DMF	2,5 HXD	CPT	2-methyl CPT	3-methyl CPT	CHX	
2	2.76	10.27	0.58	0.89	0.84	0.28	27.64
12	2.97	13.17	0.78	4.12	1.71	1.09	35.44

Table 2: Time variation for reaction with 5 wt.% glucose as feed, 10 mg 5 wt% Pd/MWCNT, temperature (200° C), pressure (1200 psi H_2). The conversion for both the reaction is 100%. DMF: Dimethyl furan; HXD: hexanedione; CPT: cyclopentanone; CHX: cyclohexanone.

3.1.3 Glucose/Fructose feed comparison

When we change feed from glucose to fructose we see an increase in mole balance. As we discussed earlier that fructose is unstable and has a lot of open chain structures which are necessary for dehydration, hence there is an increase in product yields [8]. Also, the aldol condensation/addition products of fructose are sterically hindered [8].

Feed	Yield %						Mole balance
	2,5 DMF	2,5 HXD	CPT	2-methyl CPT	3-methyl CPT	CHX	
Glucose	2.76	10.27	0.58	0.89	0.84	0.28	27.64
Fructose	4.26	21.34	0.2	1.11	0.39	0.59	36.73

Table 3: Feed variation for reaction with 5 wt% glucose/fructose as feed, 10 mg 5 wt.% Pd/MWCNT, temperature (200° C), pressure (1200 psi H_2). Conversion for both the reaction is 100% DMF: Dimethyl furan; HXD: hexanedione; CPT: cyclopentanone; CHX: cyclohexanone

3.2 HMF upgrading

As shown in table 4, various catalyst systems were tested for HMF hydrogenation. Comparing reaction 1 and 4, we see that Pd gives lower yield of product as compared to Ru. On Ru, HMF undergoes hydrodeoxygenation to 5-methyl furfural. Looking at lower product yield and no intermediate being detected we suspect that on Pd, the aldehyde group of HMF is first hydrogenated forming 2,5 bishydroxymethyl furan (BHF) (Figure 11). Due to high reactivity of BHF, it is quickly polymerized, giving us high unbalanced carbon. Ru/TiO_2 gave highest yield of products (Table 4, entry 1). HMF undergoes hydrodeoxygenation of hydroxyl group to produce 5-methyl furfural, which on further hydrogenation and deoxygenation produces 2,5 dimethyl furan. On the contrary, Ru/SiO_2 did not give any products. Even in the case of Pd metal, only Pd/TiO_2 is able to produce 2,5 Dimethyl Furan. This shows that support also play an important role for hydrodeoxygenation.

Reaction no.	Catalyst	Conversion	Yield%	
			5-Methyl Furfural	2,5 Dimethyl Furan
1	2wt% Ru/TiO_2	53.70	17.12	5.61
2	2wt% Ru/TiO_2-OTS	23.24	0.00	1.09
3	2wt % Ru/SiO_2	25.35	0.00	0.00
4	2 wt% Pd/TiO_2	28.74	0.00	1.79
5	2 wt% Pd/SiO_2	13.73	0.00	0.00
6[a]	2 wt% Ru/TiO2	50.24	0.00	2.12

Table 4: HMF hydrogenation with different catalyst system. Reaction conditions: 20 ml decalin + 15 ml THF as solvent. 50 mg catalyst. 1.3 wt% HMF as feed. Temperature (200° C), Pressure (550 psi H_2), reaction time (3 hrs.). [a] 1 ml water + 14 ml THF + 20 ml Decalin used as solvent.

As stated in the paper by Alexis T. Bell et al., TiO_2 support in the presence of molecular H_2 gas leads to the formation of oxygen vacancy as per the equation shown in figure 21 [32].

$$Ti^{4+}\text{-}O\text{-}Ti^{4+} + H_2 \rightarrow Ti^{3+}\text{-}\square\text{-}Ti^{3+} + H_2O$$

Figure 21: Equation for oxygen vacancy formation [32]

A single oxygen vacancy formed leads to formation of two reduced Ti^{3+} ions and a H_2O molecule. The concentration of these oxygen vacancy sites is more near the Ru metal cluster known as the interfacial sites [33]. In the paper by Rachel Narehood Austin et al. they have shown different mechanism for phenol hydrodeoxygenation over

Ru/TiO_2. Similar mechanism can be assumed for hydrodeoxygenation of HMF. One of the mechanism is as shown in figure 22.

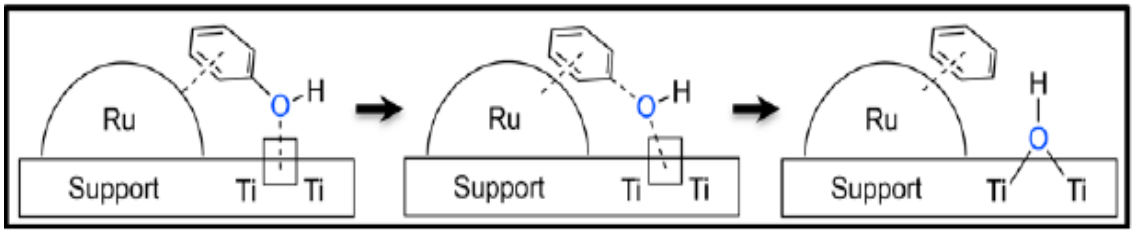

Figure 22: Mechanism for Phenol hydrodeoxygenation over Ru/TiO_2 [33]

Phenol adsorbs on Ru cluster by π-d electron interactions. The oxygen vacancy near the Ru cluster has strong affinity for oxygen. This weakens the C-O bond. The C_6H_5 adsorbed on Ru cluster undergoes easy H atom transfer from Ru cluster. By increasing the temperature of reduction of Ru/TiO_2 we can modify the number of oxygen vacancy sites [34]. This is shown in figure 23, where we increase the temperature of reduction from 200° C to 250° C. We see an increase in yield of 5-methyl furfural. Increase in product yield can also be attributed to partial reduction of Ru/TiO_2 at lower temperature. Running reaction at different hydrogenation temperature might help in explaining the effect of temperature on reduction potential of Ru/TiO_2.

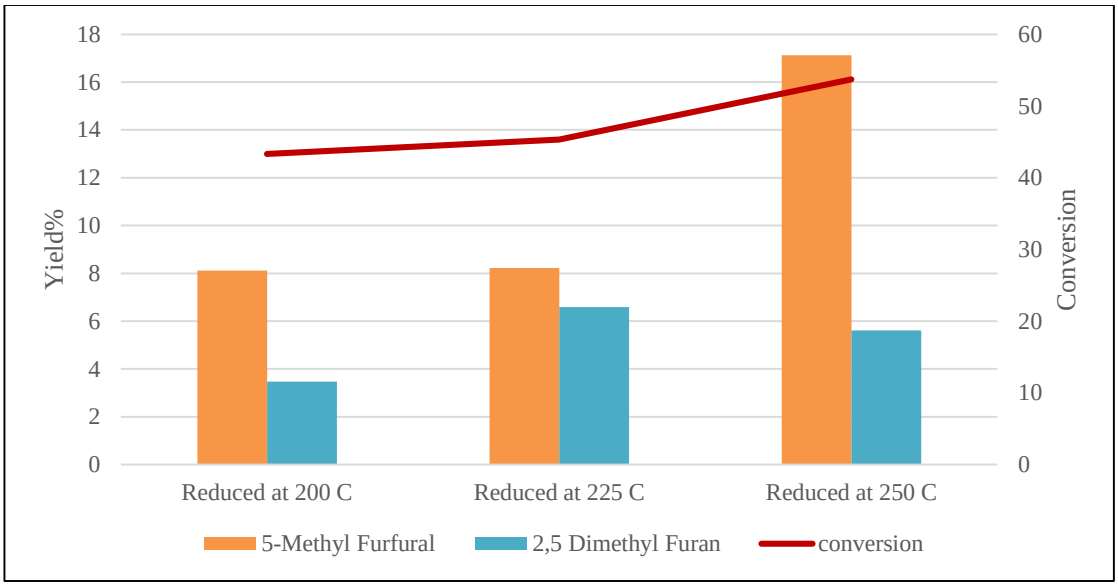

Figure 23: Varying reduction temperature of Ru/TiO_2, to test for SMSI effect. Reaction Condition: 50 mg of 2 wt% Ru/TiO_2; 20 ml Decalin + 15 ml THF as solvent; temperature (200° C); reaction time (3 hrs.); pressure (550 psi of H_2).

From figure 21, it is evident that with increasing reduction temperature of Ru/TiO_2, the yield of 5-methyl furfural increases. This confirms that dehydration is taking place at interfacial site between metal and oxide support.

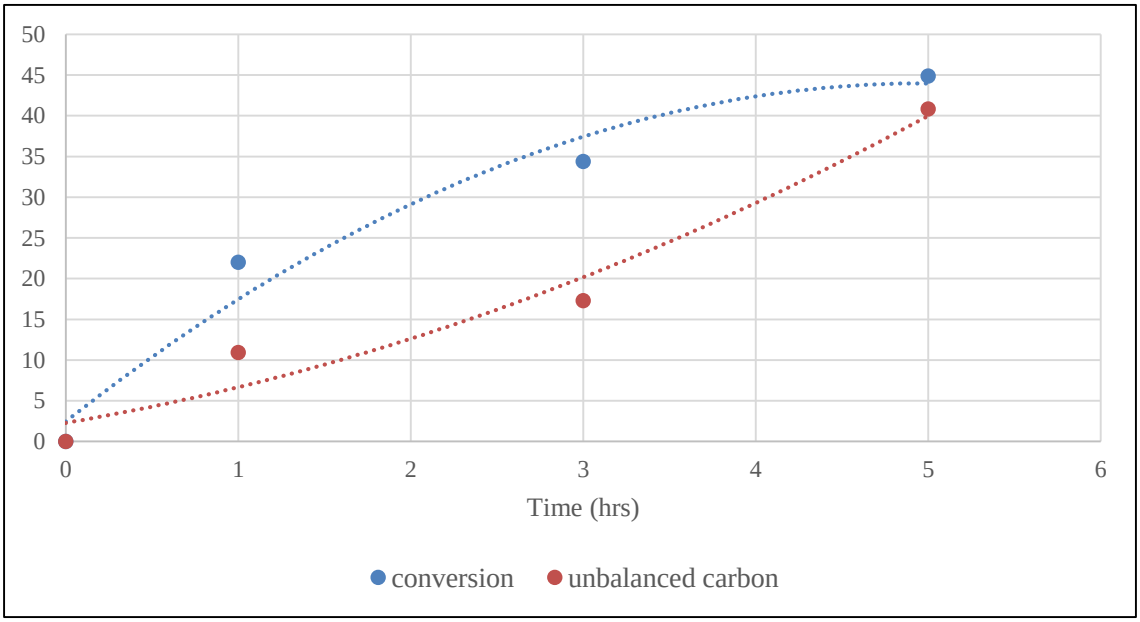

Figure 24: Conversion and unbalanced carbon variation with time for HMF hydrogenation on Ru/TiO_2. Reaction condition: 50 mg of 2 wt% Ru/TiO_2; 1.3 wt% HMF as feed; 20 ml Decalin + 15 ml THF as solvent; 200° C; 550 psi of H_2

Figure 22 and 23 plots the time variation curve for HMF hydrogenation on Ru/TiO_2. Conversion and unbalanced carbon increases with time. This indicates a

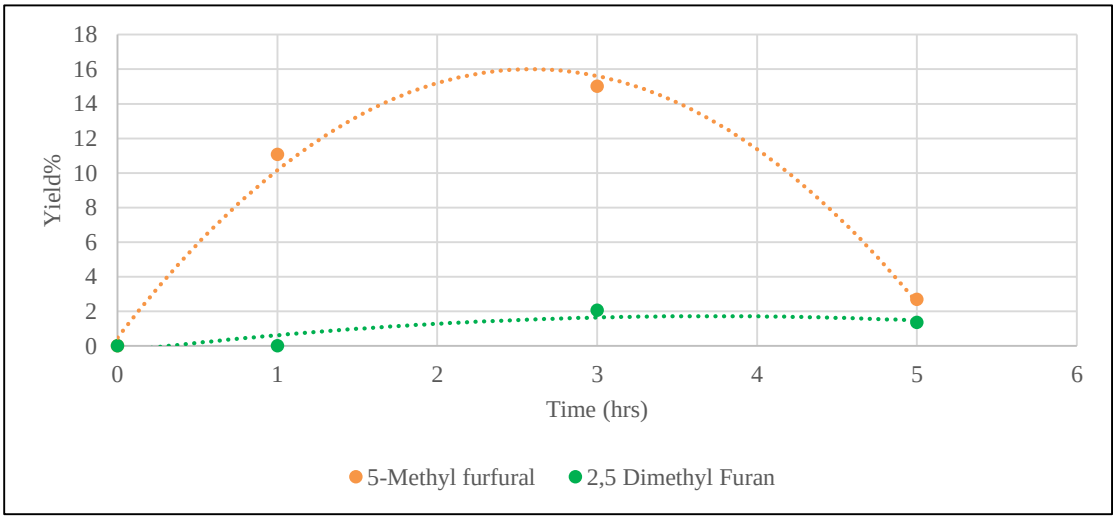

Figure 25: Product yields for HMF hydrogenation on Ru/TiO2 catalyst. Reaction condition: 50 mg of 2 wt% Ru/TiO_2; 1.3 wt.% HMF as feed; 20 ml Decalin + 15 ml THF as solvent; 200° C; 550 psi of H_2

possibility of parallel reaction to polymers. A maximum yield of 15% of 5-methyl furfural is achieved for 3 hrs. of reaction time. After 3 hrs. the yield of 5-methyl furfural drops because of polymerization of 5-methyl furfural. This phenomenon is evident when 5-methyl furfural is used as feed (appendix A, Figure 34). When 5-methyl furfural (MF) is used as feed, more unbalanced carbon is observed as compared to when HMF is used as feed. This indicates that high concentration of 5-Methyl furfural leads to its polymerization. To check for heat catalyzed degradation of HMF and 5-MF, blank reaction i.e. in the absence of a catalyst have been run at reaction conditions similar to those mentioned in figure 26. Both the compounds i.e. HMF and 5-MF did not polymerize in the absence of a catalyst. Also to check for support effect reaction with TiO_2 (P25) and HMF as feed, did not give any conversion. It was suspected that water molecule formed during the dehydration reaction of HMF to 5-methyl furfural, attacks the HMF molecule

forming polymers (humins). In order to test this hypothesis a reaction with Octadecyltrichlorosilane (OTS) functionalized Ru/TiO_2 was used, as this would help in keeping water away from catalyst surface and avoid polymerization. As shown in Table 4, entry 2, it did not give any appreciable products, which may be due to masking of active sites by long chain of OTS. In another reaction 1 ml of water was added on purpose. In table 4, on comparing reaction no. 1 and 6 it is evident that addition of water reduces the product yield. This phenomenon maybe due to humins (formed by water attack on HMF) masking the active sites, thus reducing the product yield. By varying the amount of catalyst (appendix A, Figure 35) we see that unbalanced carbon remains the same, whereas the yield of 2,5 Dimethyl furan increases. This indicates that the humins formed cover the active sites on catalyst. In the case of 100 mg of catalyst we have more number of active sites as compared to 50 mg. Hence, with 100 mg of catalyst more no. of active sites are available after humin formation for carrying out reaction, giving high yield of 2,5 Dimethyl furan.

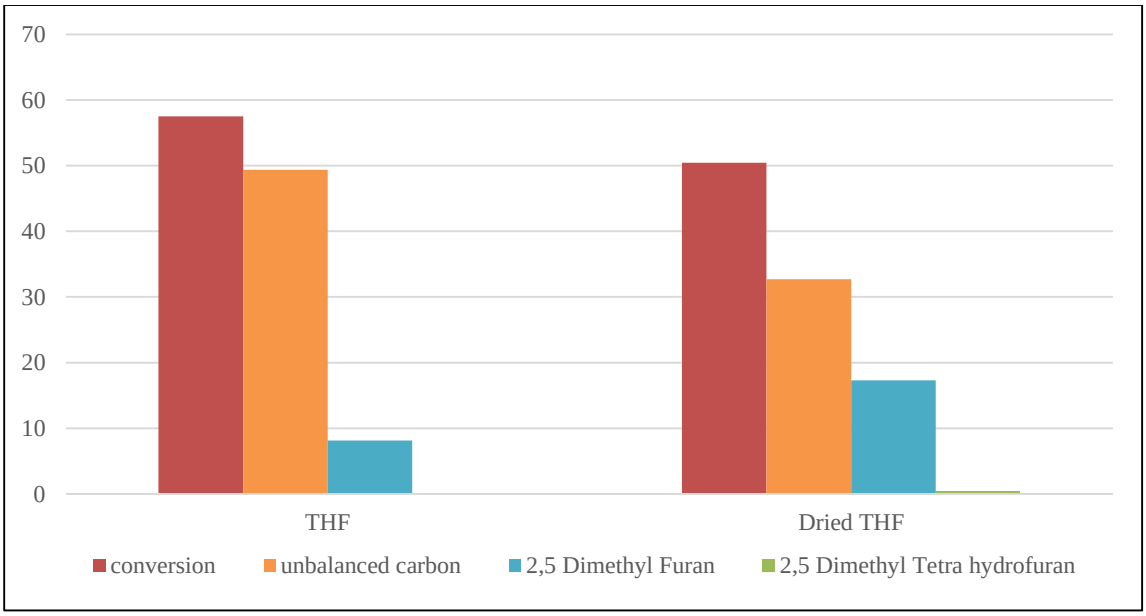

Figure 27: Conversion, Unbalanced carbon and product yield for dried THF compared to commercial THF. Reaction condition: 50 mg of 2 wt.% Ru/TiO_2; 1.3 wt.% HMF as feed; 20 ml Decalin + 15 ml THF as solvent; Temperature (200 °C); reaction time (3 hrs.); pressure (550 psi of H_2)

Figure 26: Pressure equalizer and condenser arrangement for drying THF.

As the THF solvent is hygroscopic, it might have moisture which may attack the HMF and form humins. In order to remove moisture from THF, it is stirred with CaH_2. As per the equation:

$$CaH_2 + 2H_2O \rightarrow Ca(OH)_2 + 2H_2$$

CaH_2 reacts with water molecules in THF, forming Calcium hydroxide and hydrogen. Dried THF is separated from crude THF by evaporating the crude THF at boiling point of THF i.e. 66° C and collecting the condensate in a pressure equalizer tube and condenser arrangement. Crude THF should be evaporated under observance for formation of white crystals, which indicates the formation of peroxides. In the presence of peroxides, the round bottom flask might explode with small vibrations.

Figure 25, compares the reaction with commercial THF and dried THF. We see that unbalanced carbon goes down with an increase in product yield. This again points that unbalanced carbon mask the active sites and we see a drop in product yield.

3.3 Furfural Upgrading

3.3.1 3,4 dihydropyran as feed

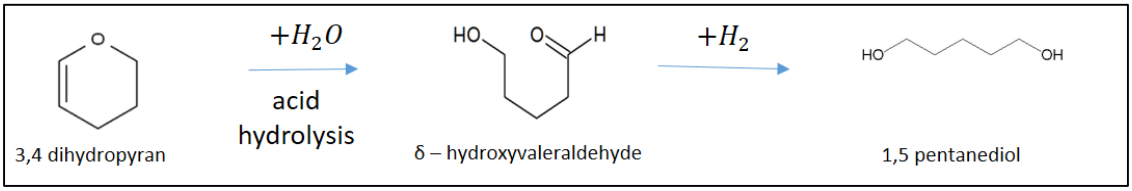

Figure 28: Reaction pathway for 3,4 dihydropyran conversion to 1,5 pentanediol

Initially, 3,4 dihydropyran was used as a feed and a bifunctional catalyst was developed that could do hydrolysis of 3,4 dihydropyran to δ-hydroxyvaleraldehyde and further hydrogenation of δ-hydroxyvaleraldehyde to 1,5-pentanediol. As hydrolysis was one of the step, water was the obvious choice for solvent. An acidic support resistant to water attack was required and hence, SiO_2-Al_2O_3 (grade 135, 475 m^2/g, average pore diameter = 5 nm) was selected as catalytic support [35]. Cu was impregnated onto SiO2-

Al_2O_3 as per the procedure shown in section 2.1.3. The time variation curve is plotted in figure 27.

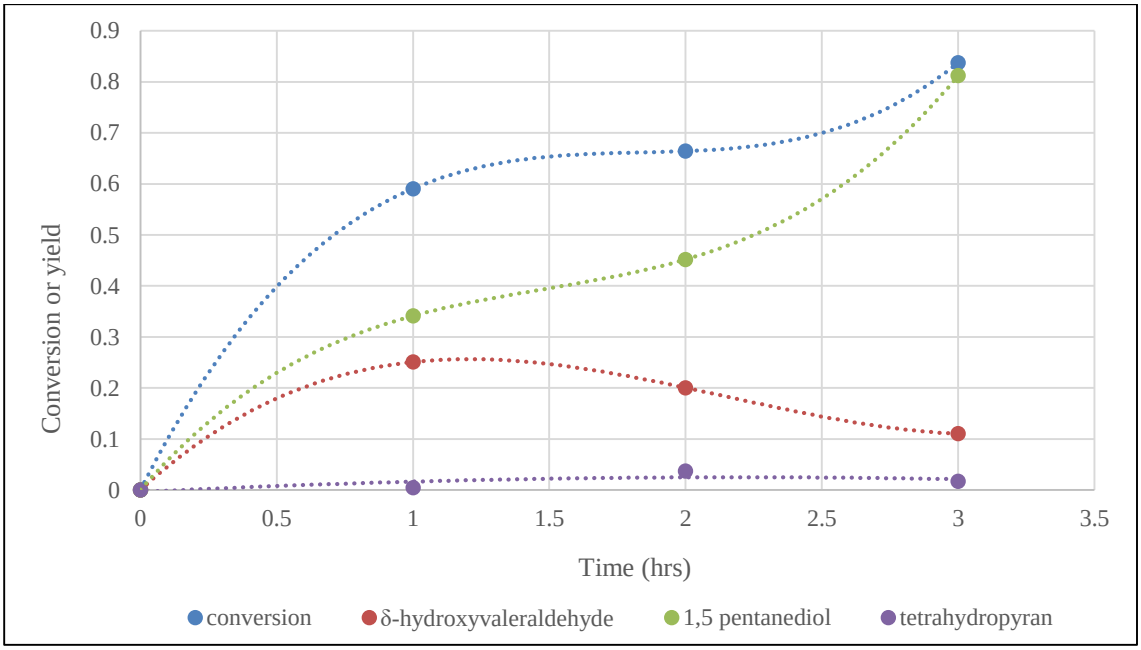

Figure 29: Time variation curve for 3,4 dihydropyran (DHP) hydrolysis and hydrogenation to 1,5 pentanediol. 100 mg 5 wt.% Cu/SiO_2-Al_2O_3. 1 wt.% DHP feed. 35 ml DI water as solvent. Reaction condition: Temperature (200° C); Pressure (550 psi, N_2).

The carbon balance for all the runs is above 95%. The curve for δ-hydroxyvaleradehyde follows a typical intermediate curve. A maximum conversion of 83% and 80% yield of 1,5-pentanediol is obtained for 3 hrs. of reaction time. We see tetrahydropyran being formed in small yields. We suspect that hydrogenation of double bond of 3,4 dihydropyran is by Meerwein Ponndorf Verley (MPV) reduction, in which hydrogen is donated from polymers or humins formed. For this we run a reaction with SiO_2-Al_2O_3. We do see the formation of tetrahydropyran in small yields. This shows that tetrahydropyran is formed by MPV reaction from polymers. This also shows that Cu is not active in hydrogenating double bond of 3,4 dihydropyran.

3.3.2 Tetrahydrofurfuryl alcohol as feed

After successfully developing and testing catalyst, 5wt% Cu/SiO_2-Al_2O_3 for 3,4 dihydropyran conversion to 1,5-pentanediol, we shifted our focus on using tetrahydrofurfuryl alcohol (THFAL) as feed and trying to convert it to 1,5-pentanediol via 3,4 dihydropyran and δ-hydroxyvaleraldehyde as intermediates (figure 14).

Using 5 wt% Cu/SiO_2-Al_2O_3 as catalyst and THFAL as feed we tested for different solvents. With increasing order of hydrophobicity, water, tetrahydrofuran and cyclohexane are solvents tested. The results are as shown in the Table 5.

Solvent	**Conversion**	**Yield%**		**Unbalanced carbon**
		3,4 dihydropyran	**Tetrahydropyran**	
Water	0%	0.00%	0.00%	0%
THF	72.47%	4.39%	13.55%	54.52%
Cyclohexane	94.77%	2.37%	5.67%	86.74%

Table 5: Testing different solvent for THFAL conversion. 100 mg 5 wt.% Cu/SiO_2-Al_2O_3; 35 ml solvent; 1.2 wt.% THFAL as feed; Reaction condition: Temperature (250° C); Pressure (600 psi of N_2); Time (2hrs).

We see that, as hydrophobicity of solvent increases the unbalanced carbon goes up. The reason for this is, with an increase in hydrophobicity of solvent, the reactant and products tend to stay on the catalyst, which leads to polymerization. Using water as solvent results in no unbalanced carbon. Also as water is required in second step (acid hydrolysis), we use water as solvent for our further reactions. As the conversion was zero for water as

solvent, we tried with stronger acid such as MCM-41-SO_3H-PTS (PTS = methoxypropyl silane).

With MCM-41-SO_3H-PTS (table 6, reaction 2) we see 3.6% of δ-hydroxyvaleraldehyde being formed. Conversion of tetrahydrofurfuryl alcohol to 3,4 dihydropyran involves dehydration of THFAL forming a carbocation, which on ring rearrangement forms 3,4 dihydropyran (figure 26).

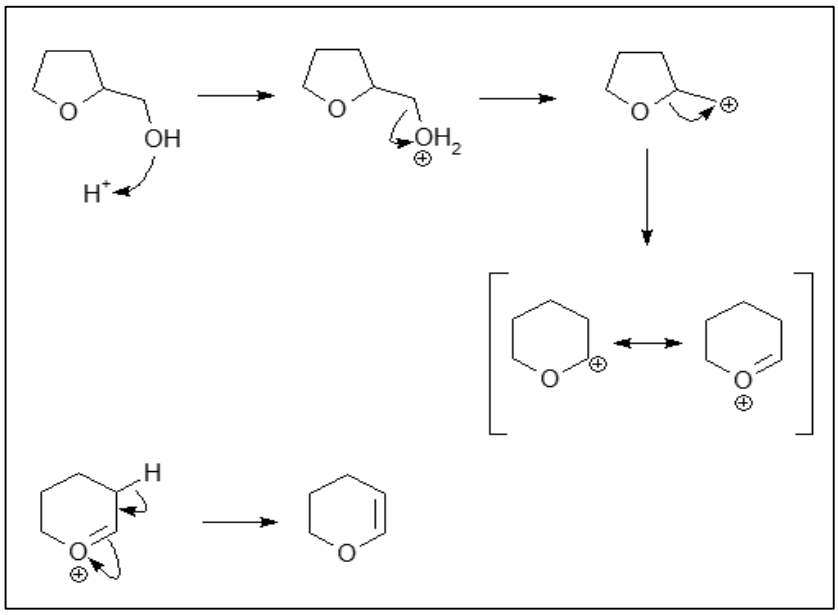

Figure 30: Tetrahydrofurfuryl alcohol conversion to 3,4 dihydropyran mechanism

We suspect that higher temperature would be required to carry out ring rearrangement efficiently. Hence, as we increase temperature from 200° C to 250° C (table 6, reaction 2 and 3), the product yield of δ-hydroxyvaleraldehyde increased from 3.6% to 8.64%. We also see 4.49% of 3,4 dihydropyran. Further increasing the temperature to 275° C increases unbalanced carbon (table6, reaction 5 and 8). Hence, 250° C is an optimum temperature.

Reaction No.	Feed	Catalyst	Temp. (°C)	Time (hrs)	Conversion	Yield%		Unbalanced carbon
						3,4 DHP	δ-HVALD	
1	1.2 wt.% THFAL	100 mg 5 wt.% Cu/SiO_2-Al_2O_3	200	2	0.00%	0.00%	0.00%	0.00%
2	1.2 wt.% THFAL	100 mg MCM-41-SO_3H-PTS	200	2	3.6%	0.00%	3.6%	0.00%
3	1.2 wt.% THFAL	100 mg MCM-41-SO_3H-PTS	250	2	17.6%	4.49%	8.64%	4.47%
4	1.2 wt.% THFAL	200 mg MCM-41-SO_3H-PTS	250	2	53.9%	6.8%	9.60%	37.5%
5	0.6 wt.% THFAL	100 mg MCM-41-SO_3H-PTS	250	2	37.03%	5.90%	14.00%	17.01%
6	0.3 wt.% THFAL	200 mg MCM-41-SO_3H-PTS	250	2	64.55%	11.10%	14.30%	39.10%
7	0.3 wt.% THFAL	No catalyst	250	2	0.00%	0.00%	0.00%	0.00%
8	0.6 wt.% THFAL	200 mg MCM-41-SO_3H-PTS	275	2	80.52%	6.5%	9.3%	64.7%
9[a]	1.2 wt.% THFAL	100 mg MCM-41-SO3H-PTS	200	2	0.00%	0.00%	0.00%	0.00%
10[b]	1.2 wt.% THFAL	200 mg MCM-41-SO3H-PTS	250 C	2	98.25%	0.00%	0.00%	96.3%

Table 6: 35 ml of water as solvent; pressure (600 psi). DHP = dihydropyran; HVALD = hydroxyvaleraldehyde
a = 35 ml THF + water (1:2) (w/w) used as solvent
b = 35 ml cyclohexane used as solvent

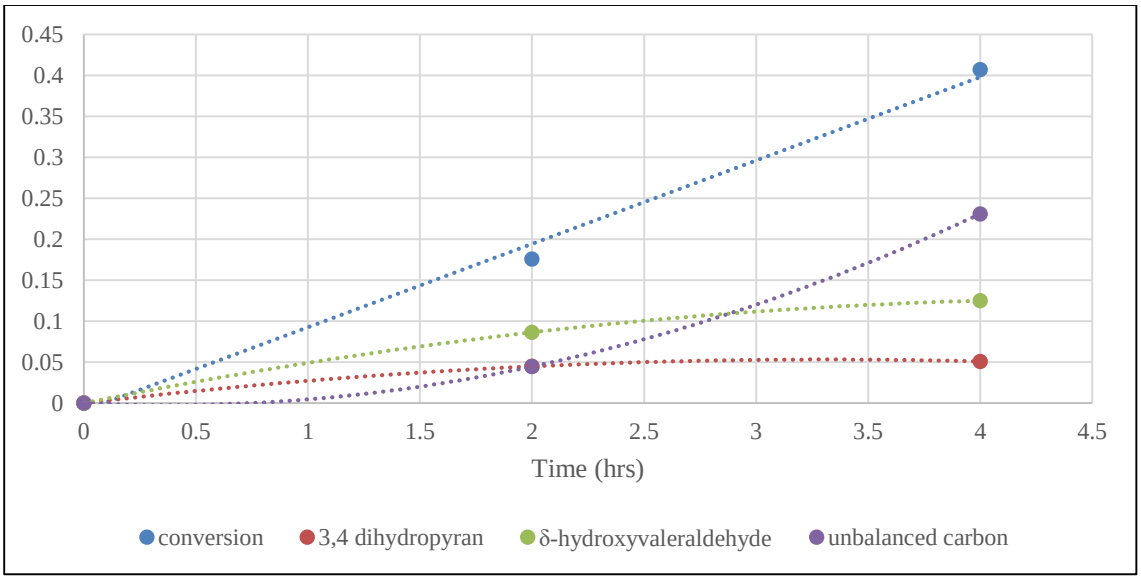

Figure 31: Time variation for THFAL as feed. Reaction condition: 35 ml DI water; 100 mg of MCM-41-SO_3H-PTS (1:1); 1.2 wt% THFAL as feed; Temp. (250° C); pressure (600 psi N_2)

Figure 29, shows time variation curves for THFAL as feed. Conversion follows straight line curve, indicating that THFAL conversion follows zero order of reaction. From 2 hrs. to 4 hrs. unbalanced carbon increases at the same rate as THFAL reacts. This shows that unbalanced carbon is majorly formed from THFAL. 3,4 dihydropyran and δ-hydroxyvaleraldehyde do not polymerize. Also, beyond 2 hrs. unbalanced carbon increases, with no appreciable increase in product yield. This may be due to humins formed covering the active sites, which deactivates the catalyst. Hence, we would use 2 hrs. time frame for our reactions.

Increasing the amount of catalyst led to an increase in unbalanced carbon with no appreciable increase in product yield (table 6, reaction 3 and 4). It is possible that by increasing the amount of catalyst we increase the rate of dehydration, but rate of ring rearrangement remains the same. This increases the no. of carbocation formed. These carbocation combines with other THFAL molecule forming ether linkage. Hence, we see

an increase in unbalanced carbon. To prove our hypothesis, we conduct an experiment by reducing the concentration of feed. This will result in reduced unbalanced carbon, as less THFAL molecule are available to form ether linkage. In table 6, on comparing reaction 4 and 5, we see that on halving the concentration of feed (feed to catalyst ratio is maintained constant), unbalanced carbon reduces and there is an increase in product yield. So, polymers being formed by ether linkage maybe correct and hence, focus should be on using low concentration of feed. Blank reaction to test for heat catalyzed degradation of THFAL was performed (table 6, reaction 7). No unbalanced carbon was observed and conversion was zero. Hence, THFAL do not polymerize due to temperature.

The reaction conditions were optimized, for minimum unbalanced carbon and maximum product yield. For 0.6 wt.% THFAL feed, 100 mg of MCM-41-SO_3H-PTS, at 250° C, for 2 hrs. an unbalanced carbon of 17.01% and product yield of 5.9% and 14% for 3,4 Dihydropyran and δ-hydroxyvaleraldehyde respectively were obtained.

The first step is dehydration of tetrahydrofurfuryl alcohol. As the solvent is water, we suspect that in order to have an efficient dehydration a mass transfer limitation for water has to be created around the catalyst. For this purpose, we run a reaction with water and THF as co-solvent in 1: 2 weight ratio (table 6, reaction 8). The conversion of THFAL is zero and a color change in reaction mixture was observed after the reaction. Also, number of small peaks were observed in FID chromatogram. This suggests that solvent, THF reacts with SO_3H groups. Cyclohexane was also used as solvent (Table 6, Reaction 10). Contrary to THF, cyclohexane gave 98.25% conversion, but majority of it went to unbalanced carbon. The reason for this is cyclohexane being hydrophobic, reactants and products tend to stay on catalyst which leads to polymerization.

3.3.3 Leaching test

Leaching test was performed to check for leaching of catalyst in water at 250° C. Reaction was performed with 200 mg of MCM-41-SO_3H-PTS at 250° C (Table 7,

Reaction No.	Feed	Catalyst	Temp. (°C)	Time (hrs)	Conversion	Yield%		Unbalanced carbon
						3,4 DHP	δ-HVALD	
1	0.3 wt% THFAL	200 mg MCM-41-SO_3H-PTS	250	2	64.55%	11.10%	14.30%	39.10%
2	Reaction mixture of rxn. 1	No catalyst	250	2	78.28%	11.7%	15.9%	50.8%
3	1.2 wt% THFAL	100 mg used MCM-41-SO3H-PTS from rxn. 1	250	2	0.00%	0.00%	0.00%	0.00%

Table 7: Leaching test results. Reaction condition: 35 ml DI water; 600 psi N_2.

reaction 1). After reaction, the catalyst was filtered and filtrate was run for another 2 hours to check for homogeneous reaction (table 7, reaction 2). We see that there is an increase in conversion, which is reflected in unbalanced carbon. There is no appreciable increase in product yield. Also, we know that THFAL is stable at 250° C i.e. there is no heat catalyzed degradation. This suggests that MCM-41-SO_3H-PTS has leached. The filtered catalyst was washed with acetone and water several times and dried in an oven overnight at 60° C. The catalyst was used again with fresh feed and solvent (table 7, reaction 3). We see the conversion is zero. There are two possibilities for this case, either the catalyst is leached 100% or it is deactivated by deposition of coke. On washing the catalyst with isopropyl alcohol, isopropyl alcohol turns pale yellow (appendix A, Figure 36) suggesting that there is deposition of humins on catalyst.

Chapter 4: Conclusion

Glucose and HMF Upgrading

An upgrading strategy to convert levoglucosan to cyclic ketones is developed. From the results of glucose upgrading, we conclude that, it is possible to convert glucose or fructose to cyclic ketones in one pot reaction. Cyclic ketones serve as good starting material for diesel range products. Further study into solvent and catalyst system would be required to get good yields of ketones.

HMF upgrading to 2,5 dimethyl furan using Ru/TiO_2 was successfully demonstrated. Hydrodeoxygenation of HMF to 2,5 dimethyl furan takes place at interfacial site between Ru metal and TiO_2 support. Number of such interfacial sites can be varied by varying the reduction temperature of catalyst. Role of water in increasing unbalanced carbon or humin formation, was also demonstrated. Caution has to be maintained to use non-aqueous dry solvent when carrying out HMF upgrading.

Furfural Upgrading

5wt% Cu/SiO_2-Al_2O_3 can successfully convert 3,4 dihydropyran to 1,5-pentanediol in a single pot reaction. A maximum 1,5-pentanediol yield of 80% is obtained at 200° C for 3 hrs. of reaction time. When using THFAL as feed, MCM-41-SO_3H-PTS gave good yield of products. Optimizing reaction conditions, product yield of 5.9% of 3,4 dihydropyran and 14% of δ-hydroxyvaleraldehyde is attained with 100 mg MCM-41-SO_3H-PTS as catalyst, 0.6 wt.% THFAL as feed, at 250° C, for 2 hrs. of reaction time. Attempts were made to modify solvent environment to make dehydration efficient. It was found that, hydrophobic solvent such as cyclohexane gave lot of humin formation and hydrophilic solvent such as THF reacted with acid group of catalyst. Solvents such as

methanol which are non-reactive to SO_3H group and hydrophobic as compared to water is recommended for use. It is also found that, increase in unbalanced carbon with time is due to polymerization of THFAL. The possible mechanism of polymerization is ether linkage formation between two THFAL molecules. It is found that MCM-41-SO_3H-PTS leaches at reaction conditions in polar solvent such as water. Further study on using a non-polar solvent is required. Catalyst can be made hydrophobic and a suitable hydrophobic co-solvent such as methanol along with water can be used to carryout dehydration efficiently. Also a biphasic reaction can be performed. The dehydration takes place in organic phase and 3,4 dihydropyran formed, is transferred to aqueous phase, where further acid hydrolysis takes place. MCM-41-SO_3H-PTS can be impregnated with Cu and THFAL conversion to 1,5 -pentanediol can be studied.

References

[1] "Overview of Greenhouse Gases," [Online]. Available: http://www3.epa.gov/climatechange/ghgemissions/gases/co2.html.

[2] "The Outlook for Energy: A View to 2040," ExxonMobil.

[3] L. Hu, L. Lin and S. Liu, "Chemoselective Hydrogenation of Biomass-Derived 5-Hydroxymethylfurfural into the Liquid Biofuel 2,5-Dimethylfuran," *Industrial & Engineering Chemistry Research,* vol. 53, no. 24, pp. 9969-9978, 2014.

[4] "Biodiesel Vehicle Emission," United States Department of Energy, [Online]. Available: United States Departmehttp://www.afdc.energy.gov/vehicles/diesels_emissions.html.

[5] H. Wang, J. Male and Y. Wang, "Recent Advances in Hydrotreating of Pyrolysis Bio-Oil and Its Oxygen-Containing Model Compounds," *ACS Catalysis,* vol. 3, no. 5, pp. 1047-1070, 2013.

[6] M. J. Prins, K. J. Ptasinski and F. J. Janssen, "Torrefaction of wood: Part 2. Analysis of products," *Journal of Analytical and Applied Pyrolysis,* vol. 77, no. 1, pp. 35-40, 2006.

[7] G. W. Huber, S. Iborra and A. Corma, "Synthesis of Transportation Fuels from Biomass: Chemistry, Catalysts, and Engineering," *Chemical Reviews,* vol. 106, no. 9, pp. 4044-4098, 2006.

[8] J. Faria, P. M. Ruiz and D. E. Resasco, "Carbon Nanotube/Zeolite Hybrid Catalysts for Glucose Conversion in Water/Oil Emulsions," *ACS Catalysis,* vol. 5, no. 8, pp. 4761-4771, 2015.

[9] M. A. Mellmer, J. M. R. Gallo, D. M. Alonso and J. A. Dumesic, "Selective Production of Levulinic Acid From Furfuryl Alcohol in THF Solvent Systems over H-ZSM-5," *ACS Catalysis,* vol. 5, pp. 3354-3359, 2015.

[10] S. Koso, N. Ueda, Y. Shinmi, K. Okumura, T. Kizuka and K. Tomishige, "Promoting effect of Mo on the hydrogenolysis of tetrahydrofurfuryl alcohol to 1,5-pentanediol over Rh/SiO2," *Journal of Catalysis,* vol. 267, pp. 89-92, 2009.

[11] B. D. (. Rolf Pinkos, P. (. Christophe Bauduin, A. P. L. (DE), D.-S. (. Gerhard Fritz and G. (. Hans Wagner, "PROCESS FOR PREPARING DELTA-VALEROLACTONE IN THE GAS PHASE". United States Patent US 2011/0237806 A1, 29th September 2011.

[12] S. Hellea, N. M. Bennett, K. Lau, J. H. Matsui and S. J. Duff, "A kinetic model for production of glucose by hydrolysis of levoglucosan and cellobiosan from pyrolysis oil," *Carbohydrate Research,* vol. 342, no. 16, pp. 2365-2370, 2007.

[13] D. Santhanaraj, M. R. Rover, D. E. Resasco, R. C. Brown and S. Crossley, "Gluconic Acid from Biomass Fast Pyrolysis Oils: Specialty Chemicals from the Thermochemical Conversion of Biomass," *ChemSusChem,* vol. 7, no. 11, pp. 3132-3137, 2014.

[14] S. Crossley and D. E. Resasco, "Molecular engineering approach in the selection of catalytic strategies for upgrading of biofuels," *AIChe,* vol. 55, no. 5, pp. 1082-1089, 2009.

[15] S. K. R. Patil, J. Heltzel and a. C. R. F. Lund, "Comparison of Structural Features of Humins Formed Catalytically from Glucose, Fructose and 5-Hydroxymethylfurfuraldehyde," *Energy Fuels,* vol. 26, pp. 5281-5293, 2012.

[16] R. Alamillo, M. Tucker, M. Chia, Y. P. Torresa and J. A. Dumesic, "The selective hydrogenation of biomass-derived 5-hydroxymethylfurfural using heterogeneous catalysts," *Green Chemistry,* vol. 14, pp. 1413-1419, 2012.

[17] N. K. Gupta, S. Nishimura, A. Takagakib and K. Ebitani, "Hydrotalcite-supported gold-nanoparticle-catalyzed highly efficient base-free aqueous oxidation of 5-hydroxymethylfurfural into 2,5-furandicarboxylic acid under atmospheric oxygen pressure," *Green Chemistry,* vol. 13, pp. 824-827, 2011.

[18] J. N. Chheda and J. A. Dumesic, "An overview of dehydration, aldol-condensation and hydrogenation processes for production of liquid alkanes from biomass-derived carbohydrates," *Catalysis Today,* vol. 123, no. 1-4, pp. 59-70, 2007.

[19] V. Fábos, L. T. Mika and a. I. T. Horváth, "Selective Conversion of Levulinic and Formic Acids to γ-Valerolactone with the Shvo Catalyst," *Organometallics,* vol. 33, no. 1, pp. 181-187, 2014.

[20] L. Hu, X. Tang, J. Xu, Z. Wu, L. Lin and S. Liu, "Selective Transformation of 5-Hydroxymethylfurfural into the Liquid Fuel 2,5-Dimethylfuran over Carbon-

Supported Ruthenium," *Industrial and Engineering Chemistry Research,* vol. 53, no. 8, pp. 3056-3064, 2014.

[21] M. Hasni, G. Prado, J. Rouchaud, P. Grange, M. Devillers and S. Delsarte, "Liquid phase aldol condensation of cyclopentanone with valeraldehyde catalysed by oxynitrides possessing tuneable acid–base properties," *Journal of Molecular Catalysis,* vol. 247, pp. 116-123, 2006.

[22] J. Ohyama, R. Kanao, A. Esakia and A. Satsuma, "Conversion of 5-hydroxymethylfurfural to a cyclopentanone derivative by ring rearrangement over supported Au nanoparticles," *Chemical Communications,* vol. 50, pp. 5633-5636, 2014.

[23] K. T. Yoshinao Nakagawa, "Production of 1,5-pentanediol from biomass via furfural and tetrahydrofurfuryl alcohol," *Catalysis Today,* vol. 195, pp. 136-143, 2012.

[24] S. Dutta, S. De, B. Saha and M. I. Alam, "Advances in conversion of hemicellulosic biomass to furfural and upgrading of biofuels," *Catalysis Science & Technology,* vol. 2, pp. 2025-2036, 2012.

[25] N. Merat, C. Godawa and A. Gaset, "High Selective Production of Tetrahydrofurfuryl Alcohol: Catalytic Hydrogenation of Furfural and Furfuryl alchol," *Journal of Chemical Technology and Biotechnology,* vol. 48, pp. 145-159, 1990.

[26] S. Koso, I. Furikado, A. Shimao, T. Miyazawa, K. Kunimoria and K. Tomishige, "Chemoselective hydrogenolysis of tetrahydrofurfuryl alcohol to 1,5-pentanediol," *Chemical Communication*, pp. 2035-2037, 2009.

[27] M. Schlaf, "Selective deoxygenation of sugar polyols to a,x-diols and other oxygen content reduced materials—a new challenge to homogeneous ionic hydrogenation and hydrogenolysis catalysis," *Dalton Transactions*, pp. 4645-4653, 2006.

[28] H. H. Geller and L. E. Schniepp, "Preparation of Dihydropyran, 8-Hydroxyvaleraldehyde and 1 $-Pentanediol from Tetrahydrofurfuryl Alcohol," *North Regional Research Laboratory*, vol. 68, p. 1646, 1946.

[29] S. Sato, J. Igarashi and Y. Yamada, "Stable vapor-phase conversion of tetrahydrofurfuryl alcohol into 3,4-2H-dihydropyran," *Applied Catalysis*, vol. 453, pp. 213-218, 2012.

[30] A. N. Bejile, "Copper based catalysts in the selective dehydration of polyols," Digital Repository @ Iowa State University, 2015.

[31] D. Liu and E. Y.-X. Chen, "Organocatalysis in biorefining for biomass conversion and upgrading," *Green Chemistry*, vol. 16, pp. 964-981, 2014.

[32] J. Strunk, W. C. Vining and A. T. Bell, "A Study of Oxygen Vacancy Formation and Annihilation in Submonolayer Coverages of TiO2 Dispersed on MCM-48," *Journal of Physical Chemistry*, vol. 114, pp. 16937-16945, 2010.

[33] R. C. Nelson, B. Baek, P. Ruiz, B. Goundie, A. Brooks and M. C. Wheeler, "Experimental and Theoretical Insights into the Hydrogen-Efficient Direct

Hydrodeoxygenation Mechanism of Phenol over Ru/TiO2," *ACS catalysis,* vol. 5, pp. 6509-6523, 2015.

[34] "Effect of Ti3+ Ions and Conduction Band Electrons on Photocatalytic and Photoelectrochemical activity of Rutile Titania for Water oxidation," *The Journal of Physical Chemistry,* vol. 120, pp. 6467-6474, 2016.

[35] M. W. Hahn, J. R. Copeland, A. H. v. Pelt and C. Sievers, "Stability of Amorphous Silica–Alumina in Hot Liquid Water," *CHEMSUSCHEM,* vol. 6, pp. 2304-2315, 2013.

[36] S. J. Tauster, "Strong Metal - Support Interactions," *Accounts of Chemical Research,* vol. 20, no. 11, p. 389, Novenber, 1987.

[37] D. E. Resasco and G. L. Haller, "INDIRECT EFFECT OF THE STRONG METAL-SUPPORT INTERACTION ON THE METAL-METAL INTERACTIONS," *Applied Catalysis,* vol. 8, pp. 99-107, 1983.

Appendix A: Supplementary Figures and Tables

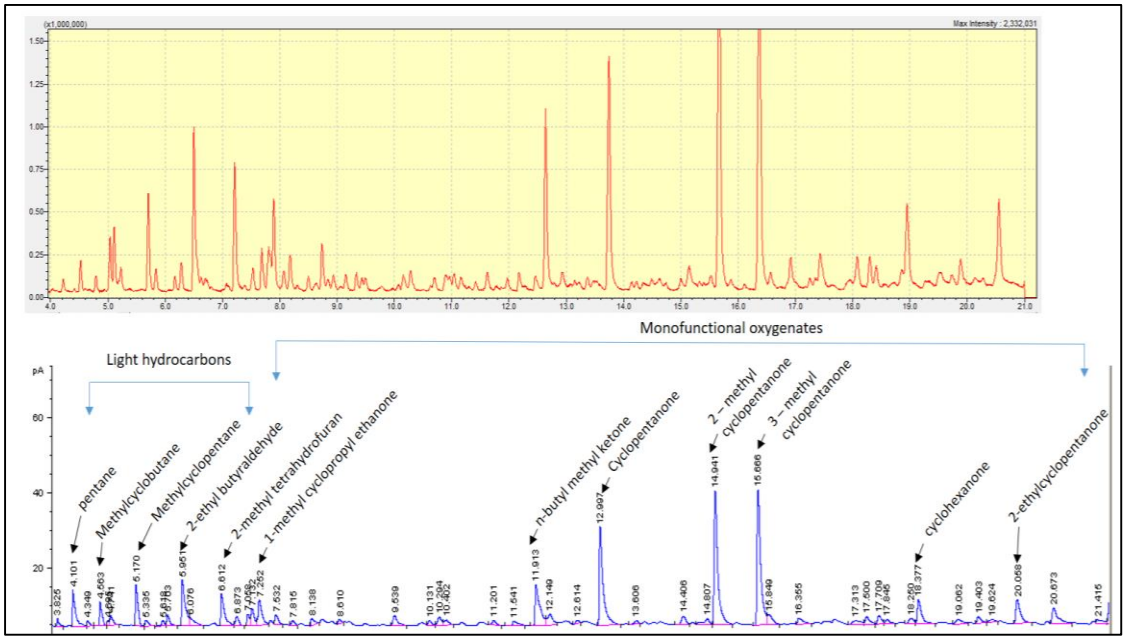

Figure 32: Organic phase analyzed in GC-MS (top) and GC-FID (bottom). The peaks are identified based on GC-MS library

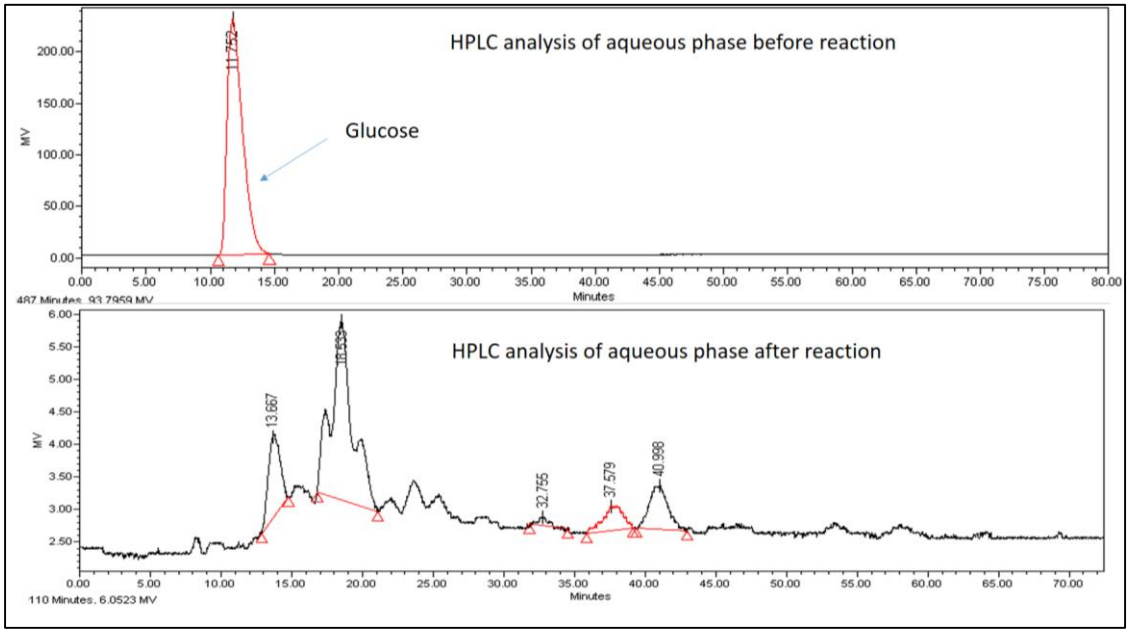

Figure 33: Aqueous phase analyzed in HPLC. Before reaction (top). After reaction (bottom). The glucose peaks disappear which means the conversion is 100%

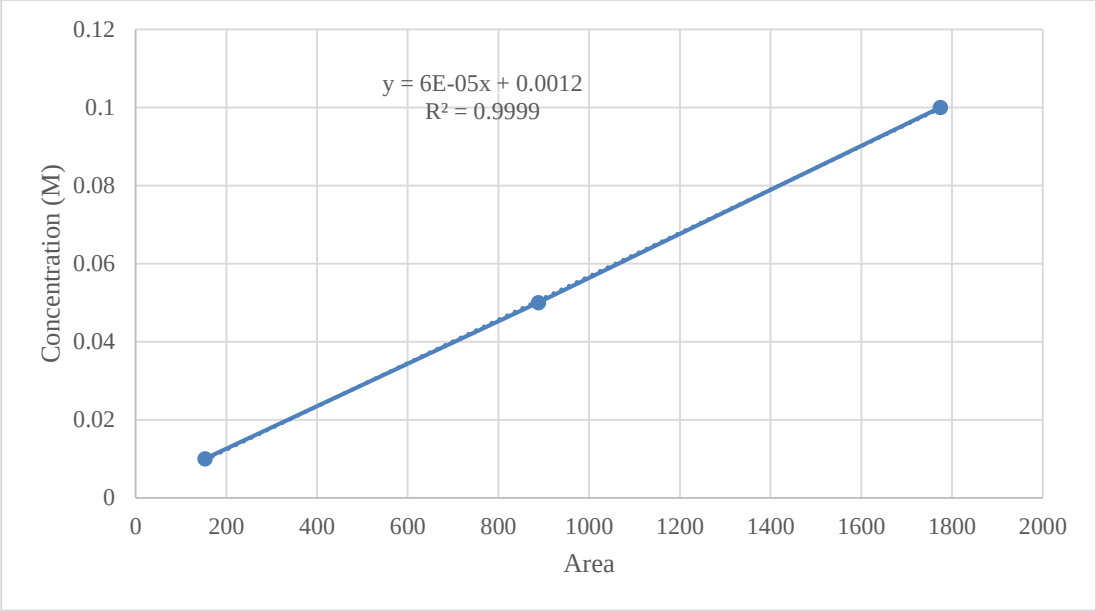

Figure 34: Cyclopentanone calibration curve

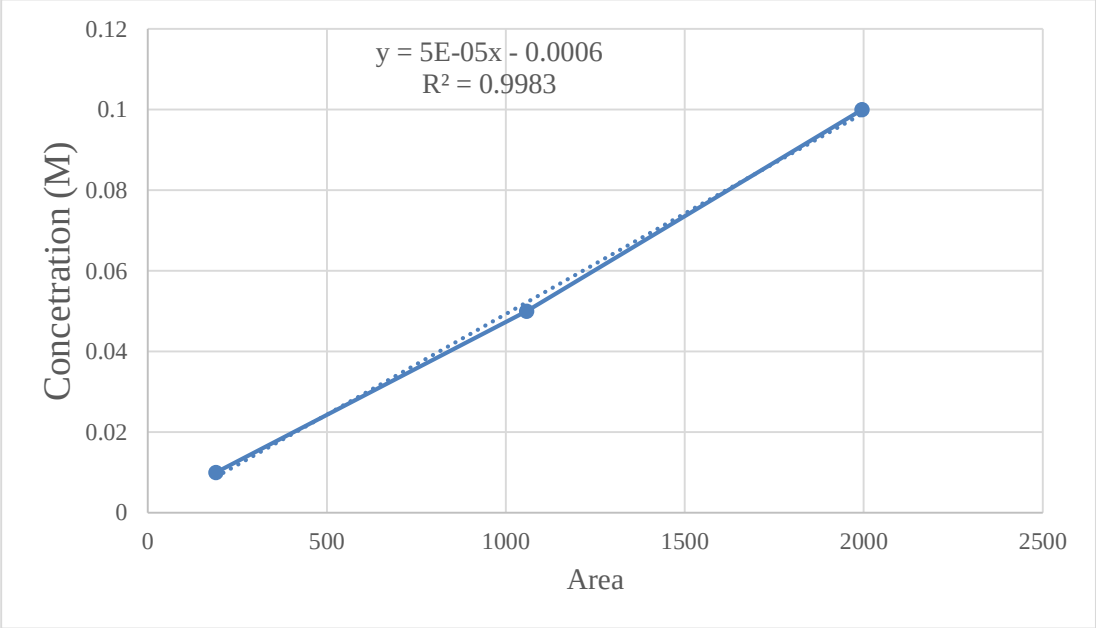

Figure 35: Cyclohexanone calibration curve

Catalyst	Yield%						Mole balance
	2,5 DMF	2,5 HXD	CPT	2-methyl CPT	3-methyl CPT	CHX	
10 mg Pd/MWCNT	2.76	10.27	0.58	0.89	0.84	0.28	27.64
10mg MWCNT+ 10mg Pd/MWCNT	3.2	10.06	0.61	0.8	0.67	0.25	27.07

Table 8: Pd leaching test. Reaction condition: 10 mg 5 wt% Pd/MWCNT, 10 ml THF, 10 ml stock solution with 35 wt% salt. 200° C, 2hrs, 1300 psi. DMF: Dimethyl furan; HXD: Hexanedione; CPT: Cyclopentanone; CHX: Cyclohexanone

Temp. (C)	Time (hrs)	Yield%							mole Balance
		2,5 DMF	2,5 HXD	N-butyl methyl ketone	CPT	2-methyl CPT	3-methyl CPT	CHX	
300	2	4.25	3.7	0	4.02	0.69	0.66	1.24	20.37
300	12	2.51	2.69	2.80	6.28	3.33	5.75	2.62	30.96
250	2	5.65	14.87	2.87	2.04	2.59	1.92	2.20	40.69
250	12	7.02	7.48	8.4	1.66	3.12	2.28	3.35	40.89
200	2	2.76	10.27	0	0.58	0.89	0.84	0.28	27.64
200	12	2.97	13.17	0	0.78	4.12	1.71	1.09	35.44

Table 9: Temperature and time variation for glucose conversion. Reaction condition: 10 mg 5 wt.% Pd/MWCNT, 10 ml THF, 10 ml stock solution with 35 wt% salt, 1300 psi H_2. DMF: Dimethyl furan; HXD: Hexanedione; CPT: Cyclopentanone; CHX: Cyclohexanone

HMF Upgrading

Feed	Conversion	Yield%			Unbalanced carbon
		5-Methyl furfural	5-Methyl furfuryl alcohol	2,5 Dimethyl Furan	
HMF	53.7	17.12	0.00	5.61	29.04
5-MF	58.9	-	0.85	10.41	40.10

Table 10: 5-(hydroxymethyl) furfural (HMF) and 5-Methyl furfural (MF) hydrogenation using Ru/TiO_2 as catalyst. Reaction condition: 50 mg of 2 wt% Ru/TiO_2; 1.3 wt.% feed; solvent (20 ml Decalin + 15 ml THF); temperature (200° C); H_2 pressure (550 psi); reaction time (3 hrs.).

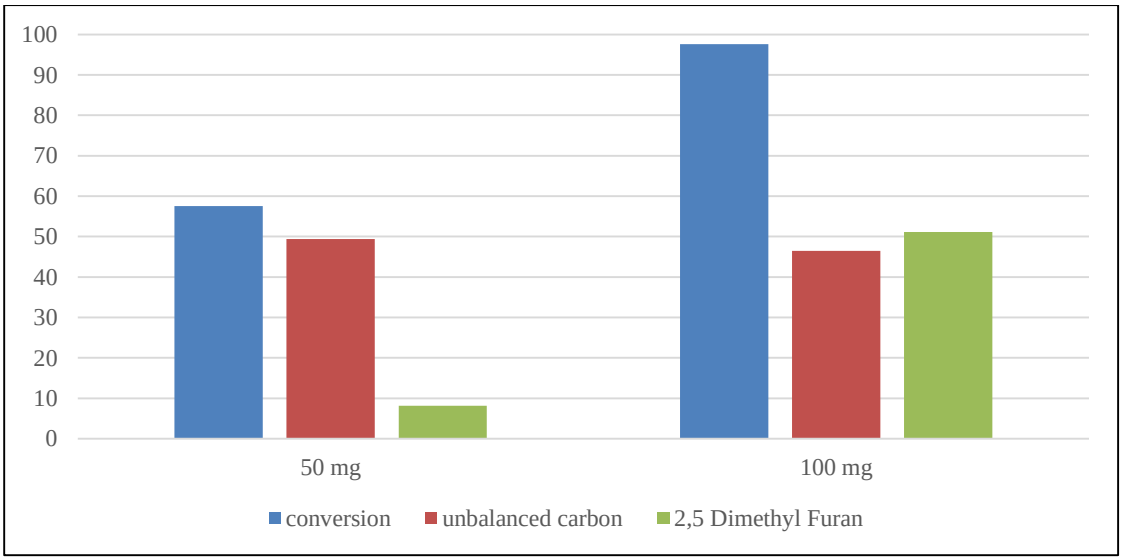

Figure 36: Catalyst amount variation. Reaction condition: 2 wt% Pd/TiO2; Feed (1.3 wt.% HMF); solvent (35 ml THF); Temperature (200° C); Pressure (600 psi of H2); Reaction time (3 hrs.)

Furfural Upgrading

Figure 37: Isopropyl alcohol solution after catalyst wash.